BROWN BEARS FACE GLOBAL WARMING

A Thesis

Presented to the

Faculty of

California State Polytechnic University, Pomona

In Partial Fulfillment

Of the Requirements for the Degree

Master of Science

In

Mathematics

By

Connor Adams

2022

SIGNATURE PAGE

THESIS: BROWN BEARS FACE GLOBAL WARMING

AUTHOR: Connor Adams

DATE SUBMITTED: Spring 2022

Department of Mathematics and Statistics

Dr. Hubertus Von Bremen _____
Thesis Committee Chair
Mathematics & Statistics

Dr. Berit Givens _____
Mathematics & Statistics

Dr. Adam King _____
Mathematics & Statistics

ACKNOWLEDGMENTS

First, I would like to say thank you to my advisor, Dr. Hubertus Von Bremen, who guided my thinking and patiently assisted me in creating this project.

ABSTRACT

Contents

List of Tables

List of Figures

Chapter 1

Introduction

Since the beginning of the 20^{th} century, global temperatures have been increasing on average, with little to no evidence of stopping [NOAA, 2022]. When the industrial revolution began, a significant amount of greenhouse gases were introduced into our atmosphere, preventing heat from escaping [EPA, 2019]. Now realizing the damage we have done to the earth, we are trying to resolve the problem without sacrificing our comfort. Unfortunately, this realization is too late for some species, such as polar and koala bears [Adams-Hosking et al., 2011, Wiig et al., 2008, Stirling and Derocher, 2012]. In this thesis, we will investigate the effects of climate change on a pair of species known to interact with each other, pacific salmon *Oncorhynchus* and Alaskan brown bears *Ursus arctos*.

Pacific salmon are sensitive to their environment and rely on sufficient river temperatures to survive spawning migration [ADFG, 2021]. Adult salmon live in the ocean, but when the time comes to reproduce, they swim up river streams to lay their eggs and usually die shortly after; this is referred to as spawning. Salmon like to begin their journey from salt water to fresh water between late

spring and early summer, but this depends on the species and location of pacific salmon [ADFG, 2021]. Specifically in Alaska, salmon can be seen spawning in river streams between the middle of July through late October [Lisi et al., 2013]. As river temperatures rise, the months in which they spawn and where they spawn may change respectively [Taylor, 2008]. Thus, global warming could potentially affect the population of pacific salmon as well as any species that interact with them.

Alaskan brown bears feed on salmon as they migrate upstream, and if the population of salmon is susceptible to changes in temperature, then the brown bears could be effected as well. Bears hibernate during winter and emerge during spring. Once emerged, they consume an enormous amount of food such as berries, roots of plants, squirrels, moose, caribou, and fish [ADFG, 2021]. Alaskan brown bears have various food sources, but salmon is currently an essential part of their diet, consuming an average of 1099 kg per year [Deacy et al., 2018, Hilderbrand et al., 1999]. Pacific salmon are already migrating further north where temperatures are more suitable for them [Taylor, 2008]. Since salmon are an essential food source for brown bears, they will probably follow salmon wherever they migrate to or replace them with a more abundant resource.

In chapter 2, we provide background information on the effects of global warming as well as the causes for the increase in the earth's climate temperature since the early 20^{th} century. We also briefly mention global temperature predictions for the next hundred years. For the remaining sections of the chapter, we review population and interaction models, such as exponential growth, logistic growth, and Lotka-Volterra equations, which will be used in the construction of our model. Lastly, we finish the chapter by introducing Theodore Modis' competitive predator-prey

model that will be the foundation for our model throughout the thesis.

In chapter 3, we introduce logistic growth models for both, the pacific salmon and Alaskan brown bear species. We begin by estimating the growth rate parameter for salmon using the reproduction rate from the Western Fisheries Research Center (WFRC) and the proportion of escapement from the National Park Service (NPS). Then, using data from the 2021 Bristol Bay annual management report, we calculate the carrying capacity by determining the maximum volume of salmon for any given run. Next, we compare growth rates from 3 different articles and calculate their average to approximate our own growth rate for the brown bear model. Lastly, we pick a carrying capacity for the brown bears using information published by the Alaskan Department of Fish and Game (ADFG).

In Chapter 4, we develop a salmon growth rate function that is dependent on time, which replaces the growth rate parameter in the salmon logistic model. We use articles by Dr. Phyllis Weber Scannell and Katherine Carter to model the proportion of salmon that survive spawning migration at different temperatures. Then, a temperature function is designed based on the changes in river temperature in Alaska for the past 30 years. Next, we use the temperature function to redesign the survival proportion model as a function of time. Finally, the proposed salmon growth rate function is constructed by combining the growth rate parameter with the survival proportion function.

We begin this chapter by introducing interaction terms, $c_{xy}xy$ and $c_{yx}xy$, which combine the salmon and brown bear growth models into a system of ordinary differential equations (ODEs). Next, a criteria is established for the parameters of the interaction terms, to ensure the behavior of the two species is similar to what we expect to observe in nature. The criteria is then used as a tool alongside the trace

and determinant of the Jacobian matrix for picking interaction parameters, c_{xy} and c_{yx}. After that, we evaluate and plot the solutions to the system of ODEs where the temperature is constant. Lastly, in this chapter, we will conclude by comparing the system of ODEs where the temperature is constant and is a function of time.

Chapter 2

Background

2.1 Climate Change

The topic of climate change has been debated for many years. Some people believe that global warming is a myth and misuse scientific research to support their claims [Allchin, 2015]. Many researchers have come to the conclusion that the earth's temperature has increased significantly since the early 20^{th} century and will continue to increase till at least the mid to late 21^{st} century [Hansen et al., 2006, Raftery et al., 2017, Osterkamp and Lachenbruch, 1990]. A group of researchers implemented a joint Bayesian hierarchical model, which determined that the global temperature will likely increase by an average of 3.2°C entering the 22^{nd} century [Raftery et al., 2017]. This significant growth in temperature is due to the increase in greenhouse gases such as carbon dioxide, methane, nitrous oxide, and fluorinated gases [Crowley, 2000, Osterkamp and Lachenbruch, 1990, EPA, 2019]. Greenhouse gases fill the air and act as a canopy that prevents heat from escaping the atmosphere, causing an escalation in climate temperature [EPA, 2019]. In

2019, the EPA reported that 80% of the earth's greenhouse gases are carbon dioxide [EPA, 2019]. Because of the high demand for transportation, electricity, industrial production, and residential/commercial use of fossil fuels, carbon dioxide will continue to be the primary source of greenhouse gas emissions [EPA, 2019]. Trees, plants, and the ocean are part of the carbon cycle which helps remove the carbon dioxide in our atmosphere. Carbon dioxide emissions have been declining slowly over the past 15 years, so there is a possibility that the global temperature trend will begin to decrease in the near future [EPA, 2019].

2.2 Logistic Growth Model

A simple equation for modeling population growth is the exponential ordinary differential equation (ODE), displayed below [Tsoularis and Wallace, 2002].

$$\frac{dx}{dt} = rx, \quad \text{where} \quad x(0) = x_0. \tag{2.1}$$

Consider $r = \text{Birth} - \text{Death} > 0$, then r is a constant that represents the growth rate of the population at any given time. Also, x is the population at time, t, so $\frac{dx}{dt}$ is the population rate of change that is dependent on t. As t increases to infinity, the population, x, will also approach infinity due to the growth being exponential. So, a more accurate way of describing population growth is using a logistic growth ODE, which is given below [Tsoularis and Wallace, 2002].

$$\frac{dx}{dt} = rx\left(1 - \frac{x}{K}\right). \tag{2.2}$$

Here, r will still represent the growth rate of the population and K is the carrying capacity. Most species follow a logistic growth pattern due to environmental constraints such as: location, food, and other essential resources. A great way to vi-

sualize K as a carrying capacity is by graphing the right hand side of Equation(2.2) as a function of x.

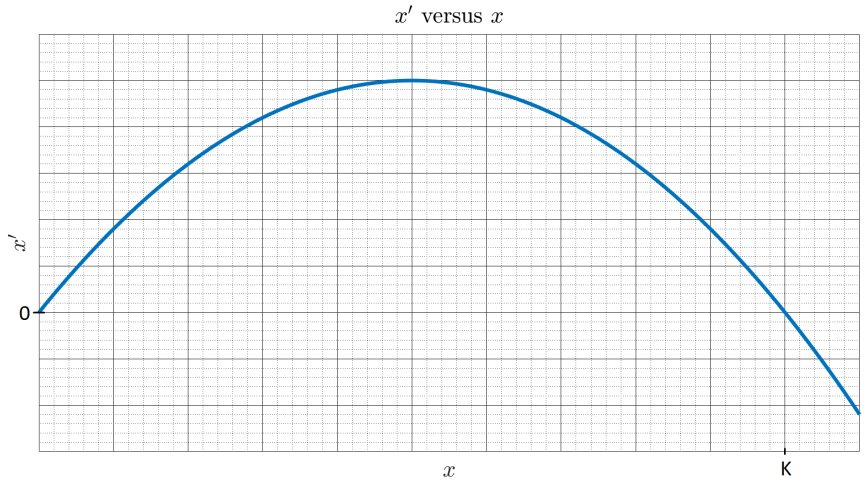

Figure 2.1: Plot of the logistic growth equation as a function function of x.

The figure above illustrates that the population, x, will continue to grow when $x < K$, but decrease when $x > K$. The population will always be converging towards K, which is what we would expect to see in the real world. Thus, the logistic model is a more accurate representation of a specie's population.

2.3 Lotka-Volterra Model

In nature, most animals share their environment, which sometimes causes species to interact, like salmon and brown bears. This relationship can be portrayed by incorporating interaction terms into each species' population equation. The interaction terms depend on both species' populations and use positive real parameters to describe the effect of one species on the other. The Lotka-Volterra model, also referred to as the predator–prey model, is a simple system of two nonlinear ordi-

nary differential equations that utilize interaction terms to imitate the relationship between two species, which is displayed below [Anisiu, 2014].

$$\begin{aligned} \frac{dx}{dt} &= \alpha x - \beta xy, \\ \frac{dy}{dt} &= \delta xy - \gamma y. \end{aligned} \tag{2.3}$$

Consider x as the prey, y as the predator, α, β, δ, and γ are positive real parameters that describe the interaction of the two species. Also, $\frac{dx}{dt}$ and $\frac{dy}{dt}$ represent the instantaneous population growth rate of each species. The interaction term for species x is subtracted from the exponential growth component, αx, to describe that the instantaneous growth rate of species x will decrease as y increases. The opposite effect happens to species y because the interaction term for species y is added instead of subtracted. The author of "US Nobel laureates: Logistic growth versus Volterra–Lotka," Theodore Modis developed a competitive predator-prey model that implements logistic growth instead of exponential, which is given below [Modis, 2011].

$$\begin{aligned} \frac{dx}{dt} &= a_x x - b_x x^2 + c_{xy} xy, \\ \frac{dy}{dt} &= a_y y - b_y y^2 + c_{yx} xy, \end{aligned} \tag{2.4}$$

where a_x, a_y, b_x, b_y, c_{xy} and c_{yx} are positive real parameters that describe the interaction of the two species.

Chapter 3

Logistic Models For The Species

Many variations of the Verhulst logistic growth model are used to illustrate the population growth of living organisms. Different variations of this model can be seen in Anastasios Tsoularis' and James Wallace's article, "Analysis of logistic growth models" [Tsoularis and Wallace, 2002]. In this thesis variations of the logistic growth model will be used in describing the populations of pacific salmon and Alaskan brown bears.

In this chapter, the logistic growth equation will be used to develop population models for both the salmon and brown bear species. Using information from the Alaskan Department of Fish and Game, we estimate a growth rate for the salmon population model. Then, we chose the carrying capacity by estimating the maximum volume of salmon for all recorded inshore runs[1] in Bristol Bay, Alaska. next, we use the average of the growth rates found in four articles to approximate the parameter, r_y, in our brown bear logistic model. Also for this model, an estimation of the carrying capacity parameter is determined based on the information provided

[1]Inshore runs are when salmon migrate back from the sea to spawn.

by the Alaskan Department of Fish and Game (ADFG).

3.1 Logistic Model For Pacific Salmon

The Alaskan rivers and streams are comprised of 5 species of salmon; sockeye *O. nerka*, chinook *O. tshawytscha*, coho *O. kisutch*, chum *O. keta*, and pink *O. gorbuscha*. Of the 5 species, sockeye salmon is the most common food source for Alaskan brown bears [Ragan, 2015]. Sockeye salmon begin their journey hatching in streams and making their way down to the ocean. At this point, they spend a year to 2 years out at sea before migrating back to the streams where they originated. According to the National Park Service (NPS), only $25 - 40\%$ of returning salmon in Bristol Bay, Alaska, escape harvesting from commercial fisheries [NPS, 2020]. They will then travel several miles upstream, where they lay and fertilize their eggs, called spawning. Salmon will then lay between 1,500 to 10,000 eggs when spawning, but only 0 to 10 of these eggs will reach adulthood [WFRC, 2022]. A significant proportion of energy for spawning salmon is spent reaching an optimal place to lay and fertilize their eggs, so much so that once they finish this process, they usually die shortly after [Ragan, 2015].

When looking at the rate for which the salmon population grows, it appears to be exponential. If on average for every salmon that lays eggs, 5 of their offspring will survive long enough to be adults ready to migrate back to their birth place. Then, according to the NPS, approximately 32% of those 5 offspring will make it past escapement to reproduce. Using this idea, the below exponential function is generated.

$$x(t) = x_0(0.32 * 5)^t, \tag{3.1}$$

where x_0 is the initial number of salmon that laid laid eggs and t represents time in years.

$$x(t) = x_0 e^{r_x t}, \tag{3.2}$$

where $r_x = \ln(0.32 * 5)$, and represents the growth rate. Now, taking the derivative of this $x(t)$ will provide the salmon population rate of change.

$$\frac{dx}{dt} = r_x x_0 e^{r_x t} = r_x x. \tag{3.3}$$

The above first order ordinary differential equation can be used in the predator-prey model, but to examine the results of it's behavior, Equation (3.2) could provide a better insight of the population trend of salmon. So, below is a plot that illustrates the growth of the salmon population with an initial starting point of 20.

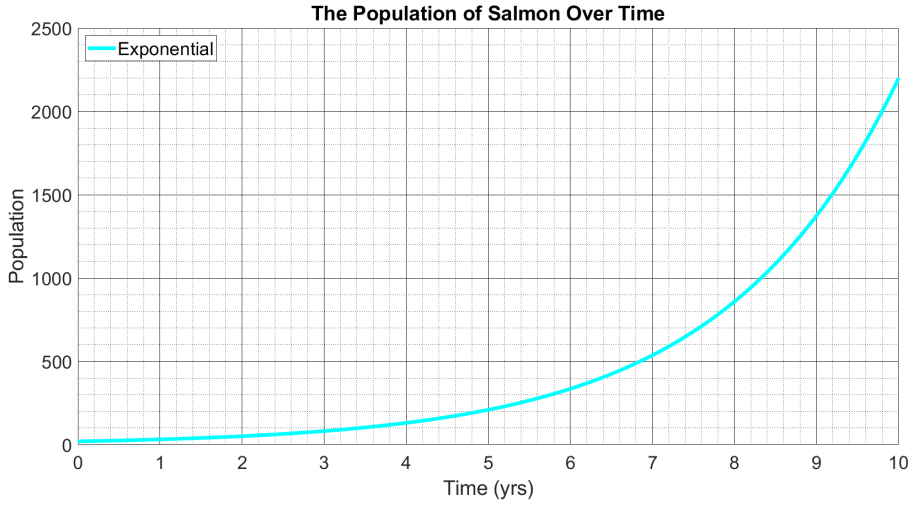

Figure 3.1: Plot of the exponential growth model for the salmon population with respect to time.

This figure illustrates that the population of salmon will increase quickly in a short time span. In just 9 years the population of salmon increases from 20 to approximately 1,400 and 1 year after this the population grows to about 2,200

which is a growth of 800 salmon. The issue with this model is the population gets extremely large in a short period of time and eventually reaches values that would fall well outside physical possibility. Since a growth rate has been established, a carrying capacity will be estimated using data from the ADFG in Bristol Bay, Alaska.

Bristol Bay is located on the easternmost side of the Bering Sea and is where a large proportion of salmon migrate to when beginning the spawning process. There was a dramatic increase in the number of sockeye salmon returning to Bristol Bay in 2021 compared to any of the previous years, but the average weight of sockeye salmon during this year decreased by a pound compared to the average of the past 20 years [Elison et al., 2022]. The sockeye species make up a large majority of the inshore runs, harvests[2], and escapements[3] in Bristol Bay each year, which explains why the brown bear population mainly feeds on sockeye salmon [Elison et al., 2022].

[2]Harvests are the number of fisheries gathered by commercial fisheries.

[3]Escapements are salmon that escape the fisheries and continues up stream to spawn.

Sockeye Comparison Between Weight and Run Size in Bristol Bay

Year	Weight (lbs)	Run (mil)
2001	6.7	22.3
2002	6.1	16.9
2003	6.3	24.9
2004	5.8	41.9
⋮	⋮	⋮
2017	5.5	57.6
2018	5.1	63.0
2019	5.1	56.4
2020	5.1	58.3
2021	4.7	67.7

Table 3.1: This table gives a brief look at the relationship between run size and the average annual weight of sockeye salmon in Bristol Bay. The complete data can be seen in Table A.1 in Appendix A.

In the first 3 years of this table the weight seems to be dramatically higher than the last 3 years, but the opposite effect appears in run size. This proposes the question that there might be a correlation between the run size and average weight of salmon each year. When taking a closer look at Table A.1 in Appendix A the trend becomes more apparent when comparing the sockeye's run size and average annual weight. Before calculating the correlation between these two events, a plot must be analyzed to see if the trend is linear.

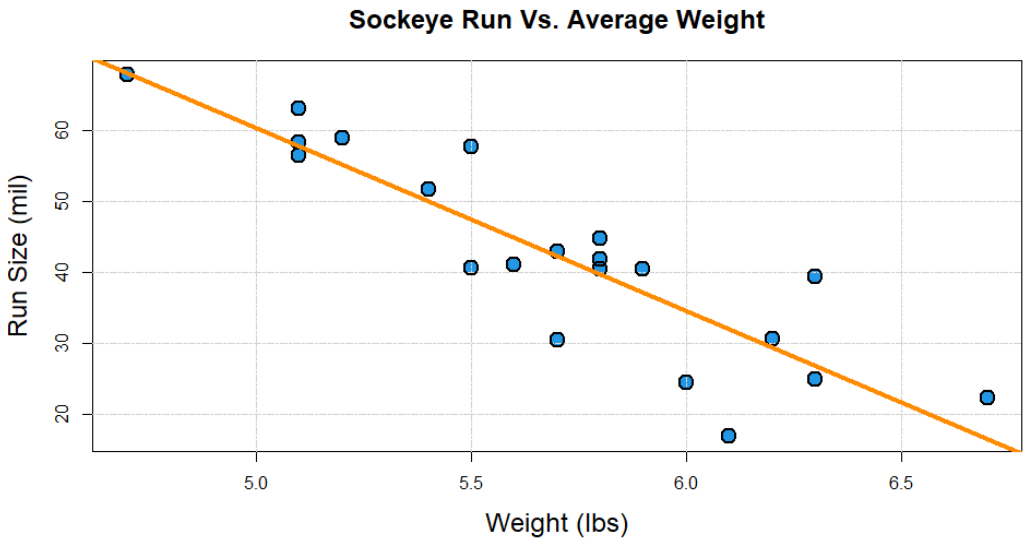

Figure 3.2: Scatter plot of the variables; inshore run size and average weight of salmon during that year's run, with the line of best fit.

Based on the figure above, there seems to be a linear correlation between sockeye run size and their average weight. The run size of the sockeye salmon decreases as the their average weight increases. Since there are multiple variables that make up the size of a salmon run each year, this helps explain the variance seen in the plot. So, calculating the correlation of these two events gives a value of -0.88. Since the correlation of these events is strong, an environmental limit of salmon can be estimated based on the maximum annual volume of sockeye salmon for the past 21 years. When looking at Table A.2 in Appendix A, the maximum volume for any given run in the last 21 years is 7.34 million cubic feet (MMCF) in 2018. The average weight of sockeye salmon during this year was 5.1 lbs which is 0.4 lbs more than the lowest average weight of 4.7 lbs in 2021. Now, the carrying capacity for sockeye salmon can be estimated using the maximum volume and lowest average weight, producing a value of 68.4 million sockeye salmon. Sockeye are not the

only salmon in the streams, but according to Table A.3 in Appendix A, they make up approximately 94% of the average annual commercial harvest in Bristol Bay. Implying that the run proportions are the same as the average annual commercial harvest, 72.8 million becomes the carrying capacity for inshore salmon runs in Bristol Bay. As stated earlier approximately 32% of theses salmon will escape commercial harvesting [NPS, 2020]. This now leaves the carrying capacity to be 29.1 million salmon each year.

Now that the carrying capacity of the salmon population has been approximated, a logistic growth model can be constructed, as seen below.

$$\frac{dx}{dt} = r_x x \left(1 - \frac{x}{K_x}\right), \tag{3.4}$$

where $K_x = 29,100,000$ is the carrying capacity, and $r_x = \ln(0.32 * 5)$ is the growth rate. If we start with an initial population of 20 million, the population should have the below trend.

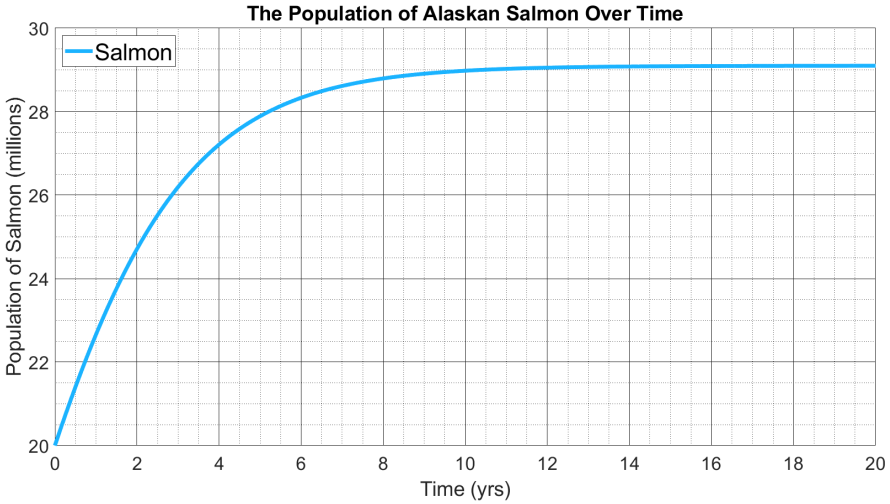

Figure 3.3: Plot of the logistic growth model for the salmon population with an initial population of 20 million.

From the graph above, the population of salmon grows rapidly for about 14 years before reaching the carrying capacity. In the next chapter, we will examine if the changes in temperature affect the growth rate of salmon, and if so, evaluate the model at different temperatures.

3.2 Logistic Model For Alaskan Brown Bears

To use the logistic growth model, the parameters r and K in Equation (2.2) have to be substituted for real values that are greater than zero. The parameter r represents the growth rate, and K represents the carrying capacity of the population. Throughout this thesis the logistic model for the Alaskan brown bear population will be displayed as the equation below.

$$\frac{dy}{dt} = r_y y \left(1 - \frac{y}{K_y}\right). \tag{3.5}$$

Researchers Lawrence J. Van Daele and Victor G. Barnes Jr. wrote a report, "MANAGEMENT OF BROWN BEAR HUNTING ON KODIAK ISLAND, ALASKA," in 2010 that discusses the growth of the brown bear population and harvest strategies to maintain a healthy species [Barnes and Van Daele, 2010]. They collected data using aerial surveys in Kodiak Archipelago and developed several models to approximate the growth rate. According to Barnes' and Van Deale's analysis of their models, the growth rate of the Alaskan brown bear population should be $r_y = 0.014$ [Barnes and Van Daele, 2010].

Van Daele and Barnes compare their results to Bruce N. McLellan's research on the dynamics of grizzly bears. McLellan's article, "Dynamics of a grizzly bear population during a period of industrial resource extraction. III. Natality and rate of increase," used the Lotka-Volterra equation to estimate the growth rate of a

grizzly bear population in Flathead Valley, Brititsh Columbia, Canada from 1979 to 1989 [McLellan, 1989]. In this article, McLellan achieves an estimated growth rate of $r_y = 0.081$. In another article, "Estimating population growth of grizzly bears from the Flathead River drainage using computer simulations of reproduction and survival rates," Frederick W. Hovey and Bruce N. McLellan have continued the research, now from 1979 to 1994, in Flathead Valley and chose a different method of estimating the growth rate on the extended data [Hovey and McLellan, 1996]. Hovey and McLellan used bootstrap for improving accuracy of estimating bias and standard error compared to the method used in McLellan's 1989 article. With the new method of calculating the growth rate and the increase in data size, Mclellan and Hovey have found similar results to Mclellan's 1989 article, where the newfound growth rate is $r_y = 0.084$.

Before comparing these growth rates, a carrying capacity for the brown bear population needs to be selected. According to the Alaska Fish & Game Department (ADFG), the current recorded population for brown bears is estimated to be 30,000 [ADFG, 2021]. From all the articles above, the common consensus is that the ADFG would like to maintain the size of the Alaskan bear population and keep it from climbing much higher than it is currently [McLellan, 1989, Hovey and McLellan, 1996, Barnes and Van Daele, 2010]. For this reason, a carrying capacity of $K_y = 45,000$ would be an appropriate estimation of the brown bears' environmental size limit. Now, for comparison, the graphs below display the solutions of Equation (3.5) for each of the growth rates.

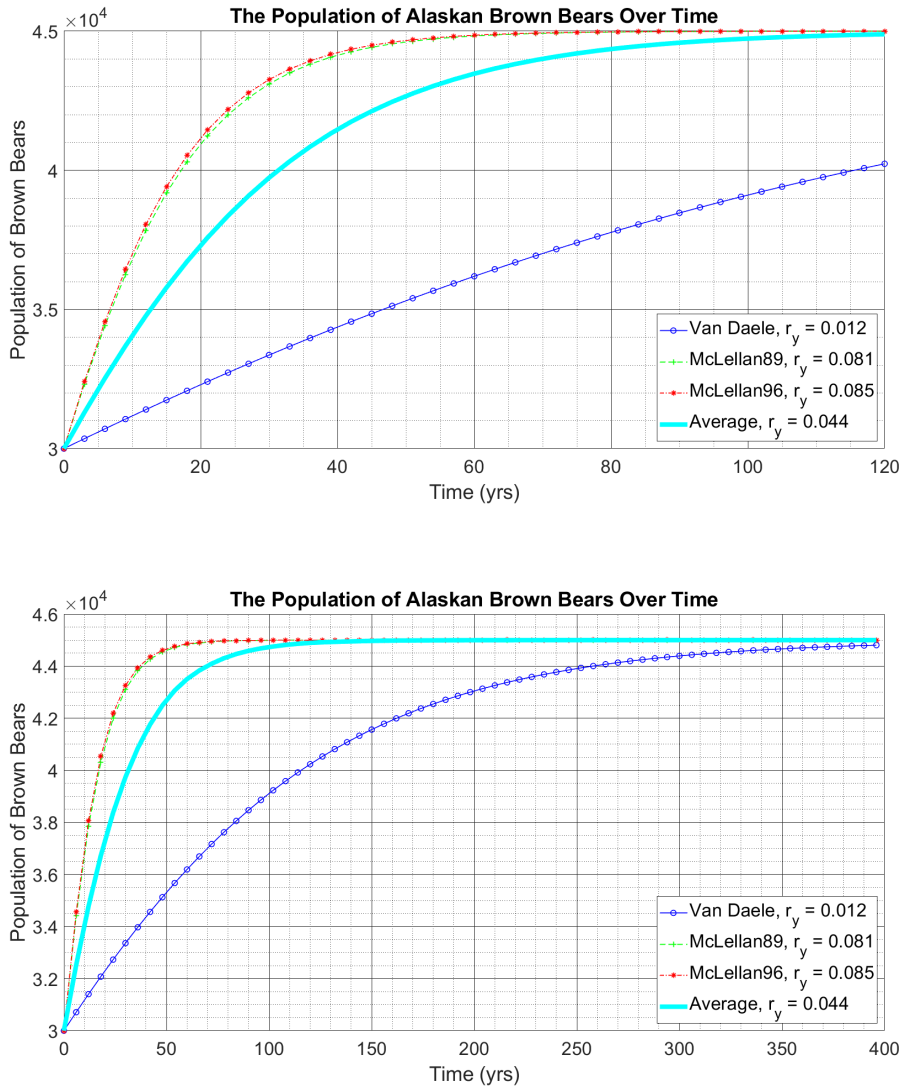

Figure 3.4: Plots of the Alaskan brown bear logistic growth equation, Equation (3.5), for each of the growth rate parameter values, r_y, discussed in the articles above as well as the average of all the growth rates. The first graph represents a time span of 120 years and the second graph represents 400 years.

In the plots above, McLellan's growth rates illustrate that the brown bear population will reach its environmental capacity within 80 years from an initial population of 30,000, while Van Daele's and Barnes' show that it would take the brown

bears approximately 400 years. For this thesis, the growth rate parameter for the brown bear population will be estimated by calculating the mean of all the growth rates discussed earlier, resulting in an estimated growth rate of $r_y = 0.044$. Figure 3.4 shows that using this growth rate would result in the brown bears reaching their environmental limit in approximately 120 years.

Chapter 4

Salmon Growth Rate Function

In this chapter, we propose a salmon growth rate function that depends on time. First, we use research articles to obtain temperatures where salmon survival during spawning migration is expected and fatal. Then, we use Katherine Carter's article, "The effects of temperature on steelhead trout, coho salmon, and chinook salmon biology and function by life stage," to extrapolate the proportion of salmon that would survive spawning migration in each of the obtained temperatures. Next, we design a function that estimates the survival proportion of salmon during spawning migration with respect to temperature. After that, we sample data from the United States Geological Survey (USGS) to construct a temperature growth model dependent on time. Then, we replace the temperature parameter in the survival proportion function with the temperature model, resulting in the function being a function of time. Lastly, we combine this function with the current growth rate parameter, which produces the proposed salmon growth rate function.

4.1 Growth Rate Function Dependent on Temperature

Salmon have an optimal temperature range for the rate at which they grow, migrate, and reproduce. If the temperature of their environment goes outside that range, then salmon may change their location of spawning, or the time when they migrate to those locations [Weber Scannell, 1992]. If they do not take either of those options, then they may fatigue and die before reaching the spawning location [Weber Scannell, 1992, ADFG, 2022]. So, when temperatures reach a critical point, mortality rates increase significantly, which consequently decreases their growth rate [Weber Scannell, 1992]. The purpose for this section is to use salmon's mortality rate during spawning migration at different temperatures to approximate a growth rate function, $R(T)$, that is dependent upon temperature. While there is little research that scientifically describe the effects of salmon population growth at each temperature, there are reports that estimate the optimum temperature range as well as critical points. Dr. Phyllis Weber Scannell wrote an amazing article in 1992 for the Alaskan Department of Fish and Game (ADFG) about the optimal temperature ranges for cold water fishes. In this article, she highlights the optimal range as well as the critical high temperature of sockeye salmon in Alaska [Weber Scannell, 1992]. Also, Katherine Carter has published an article that suggests temperatures below 2°C will result in high mortality [Carter, 2005].

Optimal Temperature Range For Pacific Sockeye Salmon

Species	**Optimal (°C)**	**Low (°C)**	**High (°C)**
Sockeye	$11 - 14$	< 2	> 22.2

Table 4.1: The optimal, critical high and low temperature range for the sockeye salmon species in Alaska [Weber Scannell, 1992, Carter, 2005].

As Dr. Scannel's report states, each researcher estimates slightly different temperature ranges due to a multitude of variables such as: acclimation, age, size, genetic strain, and physiological conditions of the fish [Weber Scannell, 1992]. That being said, we will be using Table 4.1 to help fit a curve that best illustrates the impact of temperature onto the proportion of salmon that survive the spawning migration. Now, Katherine Carter's article explains that at these critical points the population would have a 50% mortality rate [Carter, 2005]. So, under ideal conditions and optimal temperatures, 100% of the salmon population would survive the spawning migration to reproduce, and at the critical temperatures only 50% would survive. From Table 4.1 the optimal temperature range is $11 - 14$°C and the critical temperature points are at 2°C and 22.2°C, which can be observed on the graph below.

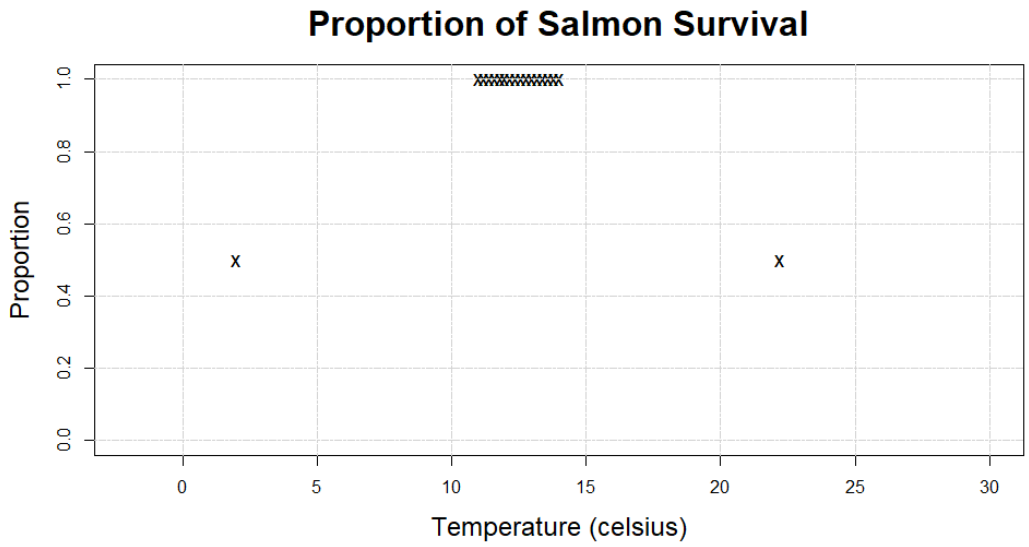

Figure 4.1: Scatter plot of the survival rates in the optimal temperature range and at the critical temperature points.

Given that the width of the optimal range is rather large, developing a function to approximate these data points will be rather difficult. The growth rate cannot drop below 0, which implies that we should be looking at a function similar to the one displayed below.

$$P(T) = \frac{1}{1 + c(T - T_{opt})^p}, \quad p \, \epsilon \, 2\mathbb{N}, \tag{4.1}$$

where $P(T)$ estimates the proportion of salmon that will survive spawning migration at a given temperature, T, in Celsius, and T_{opt} is the average of the optimal temperature range, 12.5°C. The power of the binomial, p, controls the average rate of change of the proportions, and c is a constant that will be calculated to stretch or compress the function horizontally. Now, we get the graph below by setting the parameters $p = 2$ and $c = 1$ as a starting point for the function above.

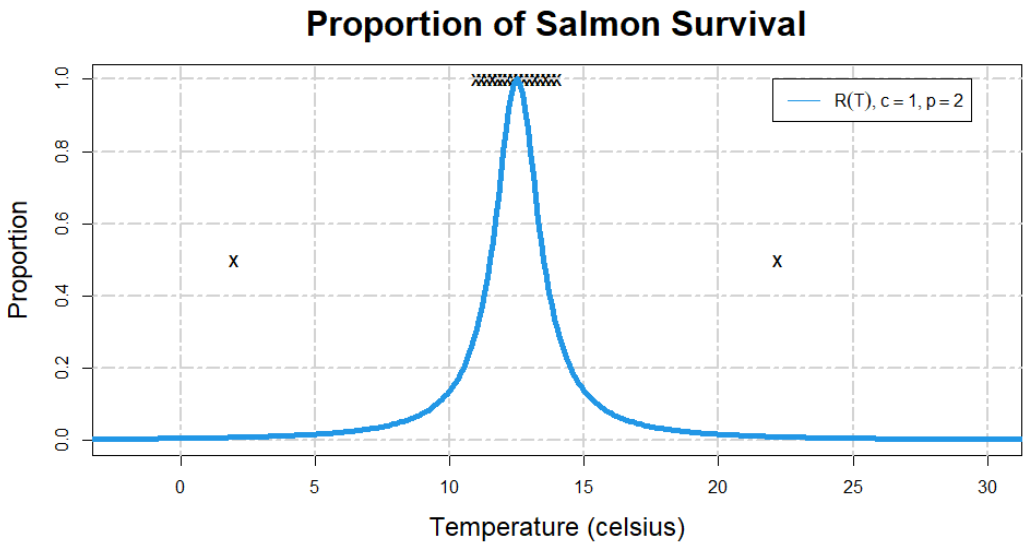

Figure 4.2: Plot of the proportion function, where $c = 1$ and $p = 2$.

The main issue with these parameters is that the peak doesn't represent the optimal range well, and the curve doesn't come close to the critical temperature points, $(2, 0.5)$ and $(22.2, 0.5)$. From the graph above, the survival proportion of migrating salmon at the limits of their optimal temperature range is $P(T = 11) = P(T = 14) \approx 0.31$, which is a major deviation from the proposed survival proportion. So, by adjusting the parameter c, we can stretch the function to better fit the survival proportions for the critical and optimal temperatures. This can be done by taking the average of the distances from T_{opt} to the critical temperatures, as shown below.

$$Avg = \frac{|T_{opt} - 2| + |T_{opt} - 22.2|}{2} = 10.1.$$

From here we can set $P(T) = 0.5$ and $T - T_{opt} = Avg = 10.1$ and solve for c.

$$c = \frac{1 - P(T)}{P(T)(T - T_{opt})^2} = \frac{1 - 0.5}{0.5(10.1)^2} = \frac{1}{10.1^2} = \frac{1}{102.1} \approx 0.01.$$

Now, plotting the $P(T)$ with parameters $p = 2$ and $c = 0.01$ produces the plot

below.

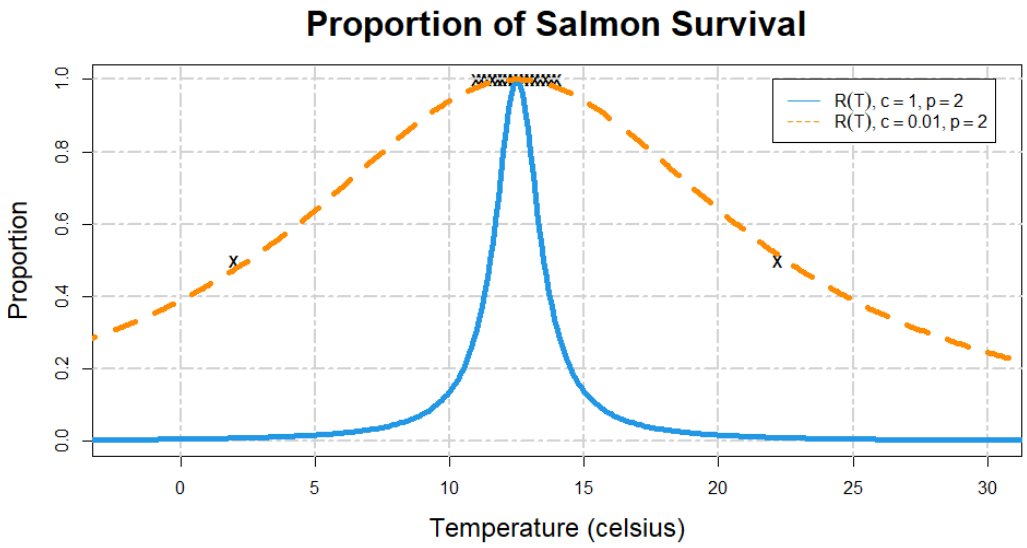

Figure 4.3: Compares the plots of the proportion function, where $c = 1$ and $c = 0.01$, but $p = 2$ remains the same.

From the figure above, the low and high critical temperature points are better represented with the new parameter, $c = 0.01$. However, at the limits of the optimal temperature range, the survival proportion is 0.978, which should be closer to 1. This can be resolved by changing the power of the binomial, $p = 2$, in Equation (4.1) to $p = 4$, which will widen the curve while maintaining a steep decent as the temperature escapes the optimal region. So, substituting the new parameters, $c = 0.01$ and $p = 4$, the graph below is produced.

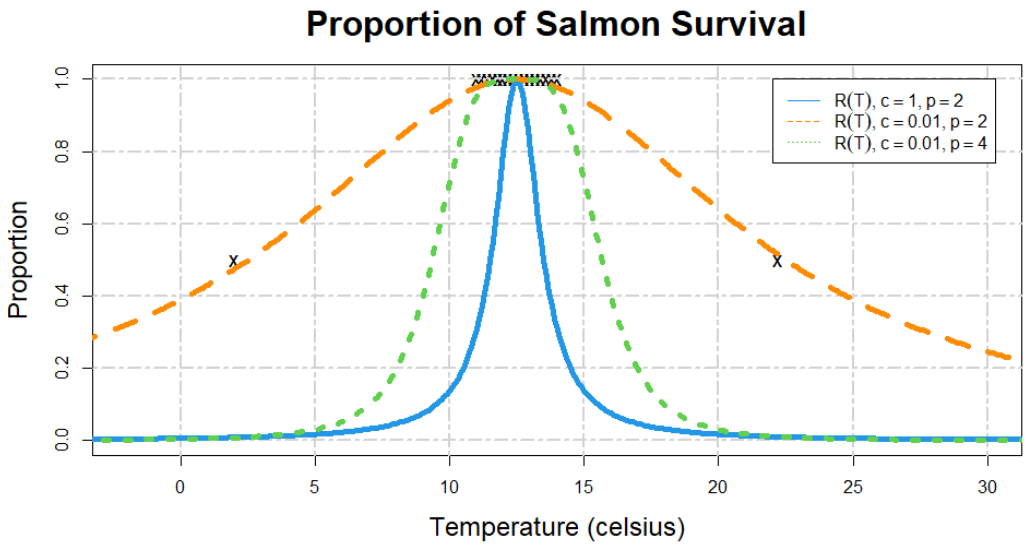

Figure 4.4: Compares the plots of Figure (4.3) with the plot of the proportion function, where $c = 0.01$ and $p = 4$.

With this figure, the representation of the optimal range is better, but the proportions of salmon survival decrease significantly as T approaches the limits of the optimal range. Also, the survival proportions at the critical temperatures are far from the points, $(2, 0.5)$ and $(22.2, 0.5)$. To resolve this issue, we can repeat the same process as earlier to select a new c value that will accurately reflect the proportions at the optimal and critical temperatures. In result, the graph below is produced by substituting the new parameter $c = 10^{-4}$ into the proportion function.

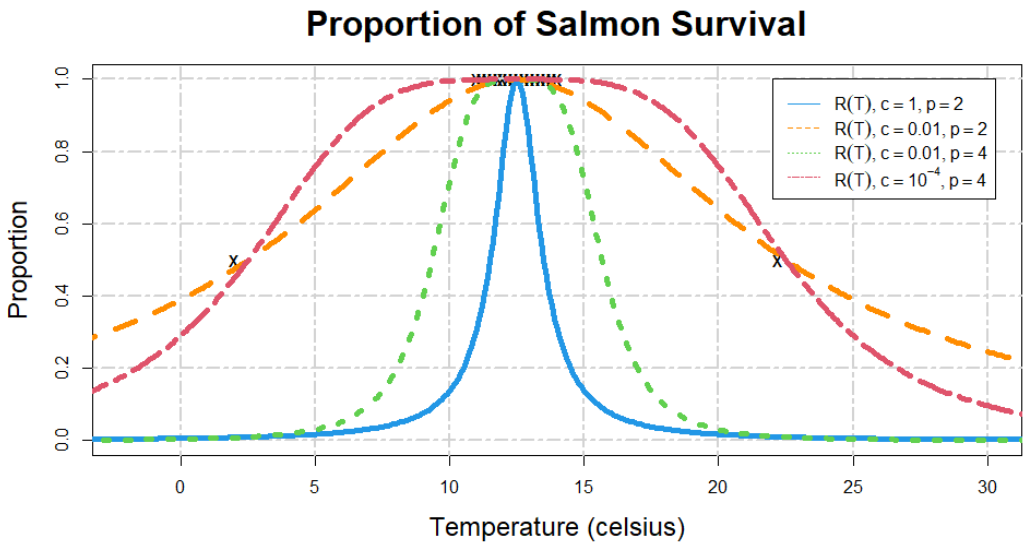

Figure 4.5: Compares the plots of Figure (4.4) with the plot of the proportion function, where $c = 10^{-4}$ and $p = 4$.

The parameters, $c = 10^{-4}$ and $p = 4$, offer a better fit, with the survival proportion being 0.9995 at the optimal temperature limits and $P(2) \approx 0.45$ and $P(2) \approx 0.53$. Now, during the salmon migration of 2004, Weaver Creek sockeye salmon experience a drastic rise in water temperature, which resulted in a higher than usually mortality rate [Farrell et al., 2008]. According to Anthony P. Farrell, temperatures were around 20.4°C and that 30% of the salmon population did not make it to the spawning location due to the excessive heat [Farrell et al., 2008]. So, using parameters $c = 10^{-4}$ and $p = 4$ in Equation (4.1) we get $P(20.4) = 0.7197$. Therefore, we estimate a 72% survival rate, or a mortality rate of approximately 28%, for the salmon migrating to their spawning locations, which is close to Anthony P. Farrell's estimation of 30%.

Looking back, the growth rate, $r_x = \ln(0.32 * 5)$, was estimated when temperatures were ideal, or in the optimal range, so combining the proportion function

with the current growth rate, we get the function below.

$$R(T) = \ln(0.32 * 5 * P(T)) = \ln\left(\frac{0.32 * 5}{1 + c(T - T_{opt})^4}\right), \tag{4.2}$$

where $c = 10^{-4}$, $T_{opt} = 12.5°\text{C}$, and T is temperature. Lastly, we will replace the growth rate, r_x, with the growth rate function, $R(T)$, in Equation (3.4) to get the below equation..

$$\frac{dx}{dt} = R(T)x\left(1 - \frac{x}{K_x}\right). \tag{4.3}$$

To see the affect of temperature on the salmon population, we will compare Equation (4.3) at different temperatures.

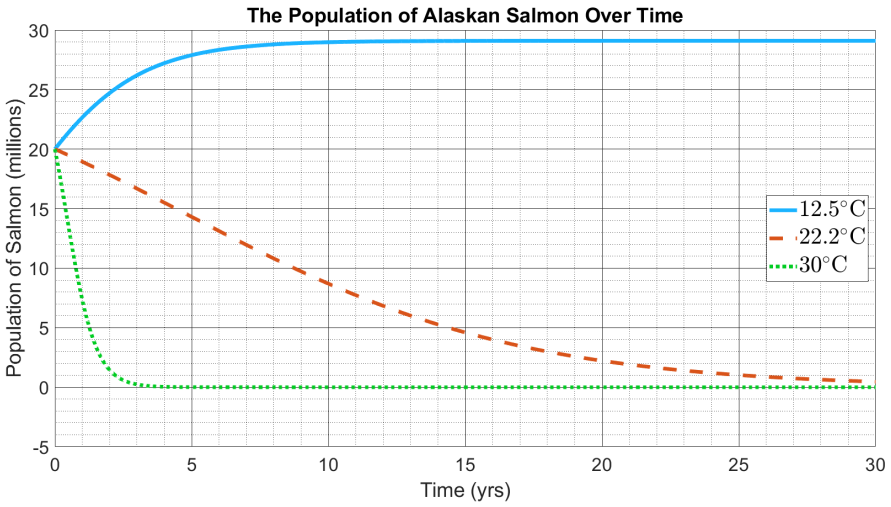

Figure 4.6: Plot of the salmon logistic growth model using the growth rate function, Equation (4.3), at 3 different temperatures.

Notice, at the optimal temperature, $T = 12.5°\text{C}$, the curve is the same as in Figure (3.3) because $R(12.5) = r_x = 0.47$. As the temperature moves further away from the optimal temperature, the reproduction of salmon is negatively affected, resulting in a decay rate, which can be observed in the middle and bottom curves. When $T = 22.2°\text{C}$ the growth rate is $R(22.2) = -0.1641$, which is explains why the

population is decreasing over time. Notice, as the temperature moves drastically far away from the optimal temperature, $T = 30°\text{C}$, the growth rate changes to $R(30) = -1.8698$, causing the population to die off in about 5 years. By replacing the growth rate of salmon with a function dependent upon temperature, we can see the drastic effects on the salmon population as temperature changes.

4.2 Temperature Function Dependent on Time

The global temperature of the earth has been growing exponentially over the past 100 years [Crowley, 2000]. Temperatures are expected to keep growing faster for at least the next 30 years [UA, 2016], unless changes are made now to the output of greenhouse gas emissions [UCAR, 2022]. Below is a graph illustrating the annual deviation of global surface temperature from the 20^{th} century average of 13.9°C.

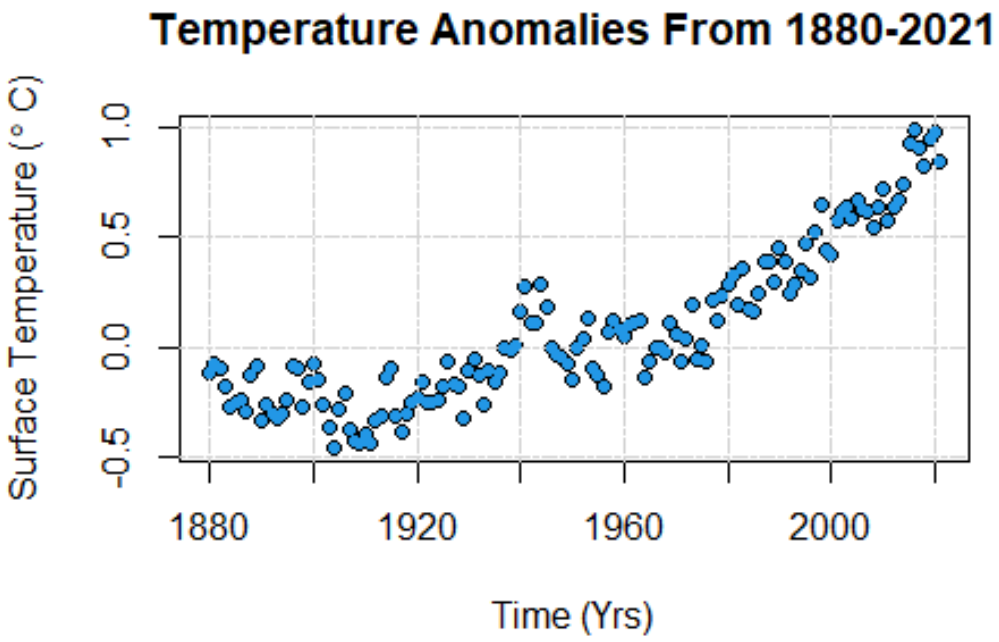

Figure 4.7: Scatter plot of the average annual global temperatures compared to the 20^{th} century average.

The data for the plot above comes from the National Oceanic and Atmospheric Administration (NOAA) [NOAA, 2022]. Any of the points below 0°C represent the years in which the temperatures were less than 13.9°C, and the points above 0°C the represent years were the temperatures were greater than 13.9°C. Judging from the plot above there seems to be some sense of slowing down after 2010 which aligns with statements made by the EPA, that there has been a recent reduction in the emissions of carbon dioxide [EPA, 2019]. The graph above shows that the earth's temperature decreases from 1880 till about 1910 before increasing almost exponentially to the present. Starting around 1970 to the present the data appears to have linear growth. While an exponential regression model can be used to fit the

data, a quadratic model would seem to work better because of the initial decrease from 1880 to 1910. The quadratic model would look like:

$$T(t) = at^2 + bt + c, \tag{4.4}$$

where $a = 7.95 * 10^{-5}$, $b = -30.25 * 10^{-2}$, and $c = 287.57$. The response variable, $T(t)$, represents temperature with the units, °C, that is dependent on time, t, expressed in years. This function seems to fit the data well with the graph below.

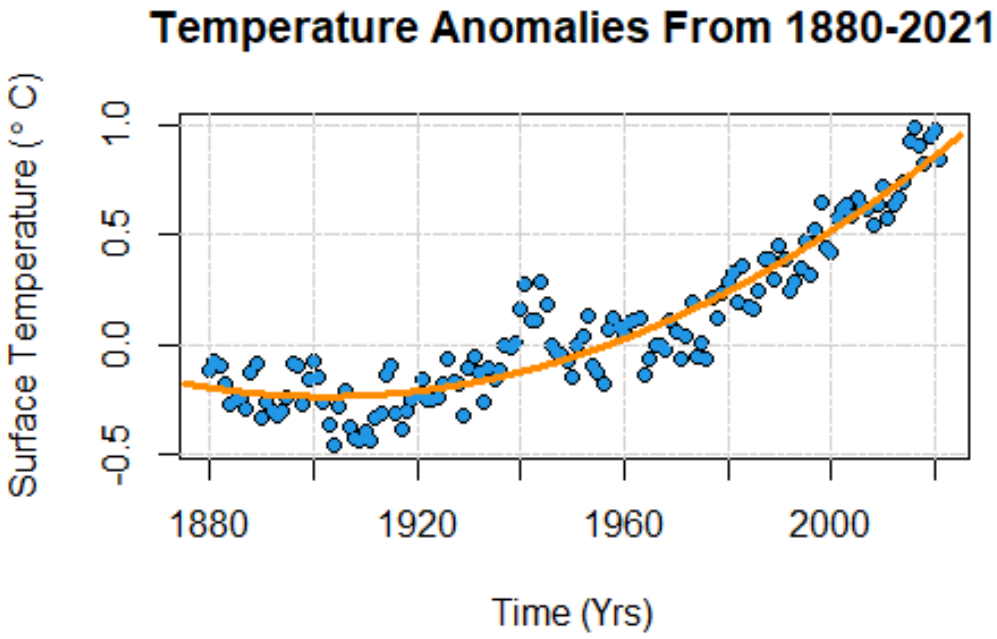

Figure 4.8: Plot of the quadratic function, $T(t)$, on top of the scatter plot given in Figure 4.7.

There is a possible issue that should be explored before continuing. This model projects the change in global temperatures of the earth, but salmon live in the ocean. So, designing a model to fit the earth's temperature might not accurately reflect

the environmental temperatures of this species. Luckily the National Oceanic and Atmospheric Administration also have data on the global sea surface temperature over the same time period [NOAA, 2022]. Below is a graph looking at the global sea surface temperature anomalies with respect to the 20^{th} century average of 13.9°C.

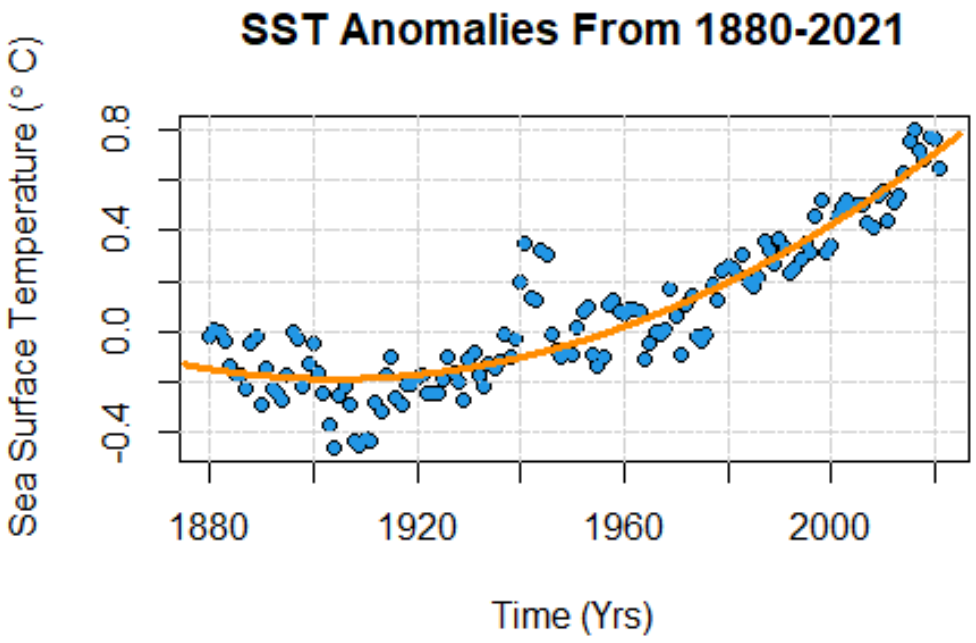

Figure 4.9: Scatter plot of the average annual sea surface temperatures compared to the 20^{th} century average, that is fitted with the quadratic function, $T(t)$, with new coefficients.

Since the graph above has a similar trend to Figure 4.7, a quadratic model seemed to fit this data well. The new parameters for the quadratic model are, $a = 6.67 * 10^{-5}$, $b = -0.25$, and $c = 241.53$. Looking at Figure 4.9, after 1970, the trend begins to appear linear, which means the quadratic equation may not be the best choice for predicting temperature. Because of this, we will look at sea surface

temperatures (SST) after 1970. Also, Alaska is ranked 40^{th} in the nation with total greenhouse gas emissions, which may effect that region's SST trend differently then other regions [ADEC, 2018].

Alaska is littered with river streams, but salmon can be seen predominately in the south parts of Alaska, such as Anchorage, Kenai peninsula, near Juneau, and Alaska Peninsula [ADFG, 2021]. According to the ADFG, salmon can be seen in these streams from June to September [ADFG, 2021]. Therefore, we will sample water temperatures in these regions during these months to model the change in temperature over time. The data was provided by the United States Geological Survey (USGS) [USGS, 2022].

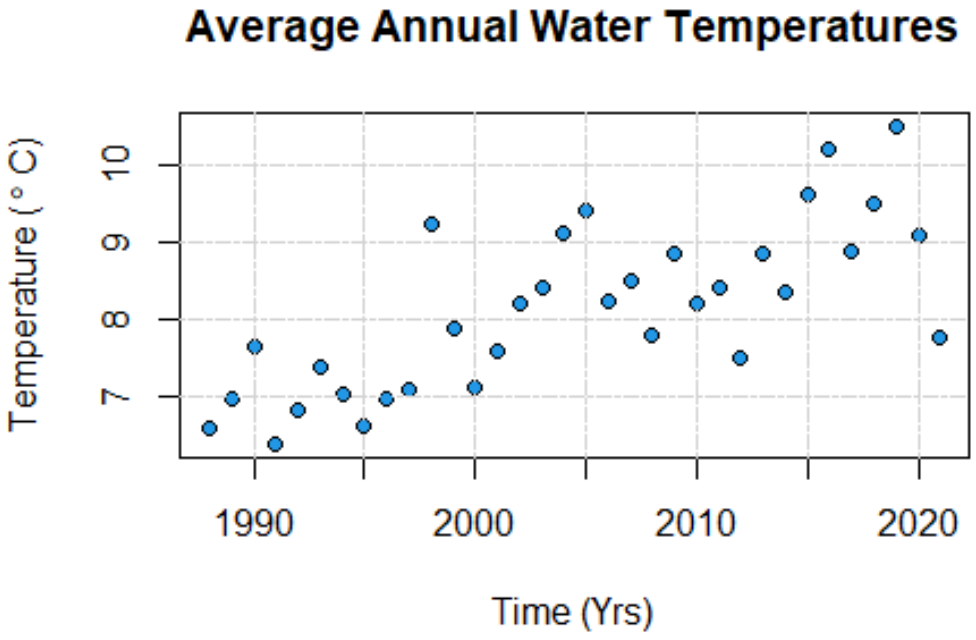

Figure 4.10: Scatter plot of the average annual water temperatures during the months of June to September in Alaska river streams.

Viewing the graph above, a linear regression model would fit the data well. When using the USGS database, there were plenty of streams where the Alaskan government was collecting data, but there were a few issues when looking at the data sets for some of the streams [USGS, 2022]. First, most data sets were a small duration of a few years, so that wasn't enough time to model a trend. Second, some data sets were missing data for a couple months every year or even just had big gaps for several years. In the end, only 5 data sets were usable for analyzing trend over time. The 5 streams used for this analysis are Cooper Creek on the Kenai Peninsula, Kenai River at Cooper Landing, Russell Creek on the Alaska Peninsula, Terror River, just south of the Alaska Peninsula, and Staney Creek which is south of Juneau. Below are the plots of each stream fitted with a linear model that closely represents their trend.

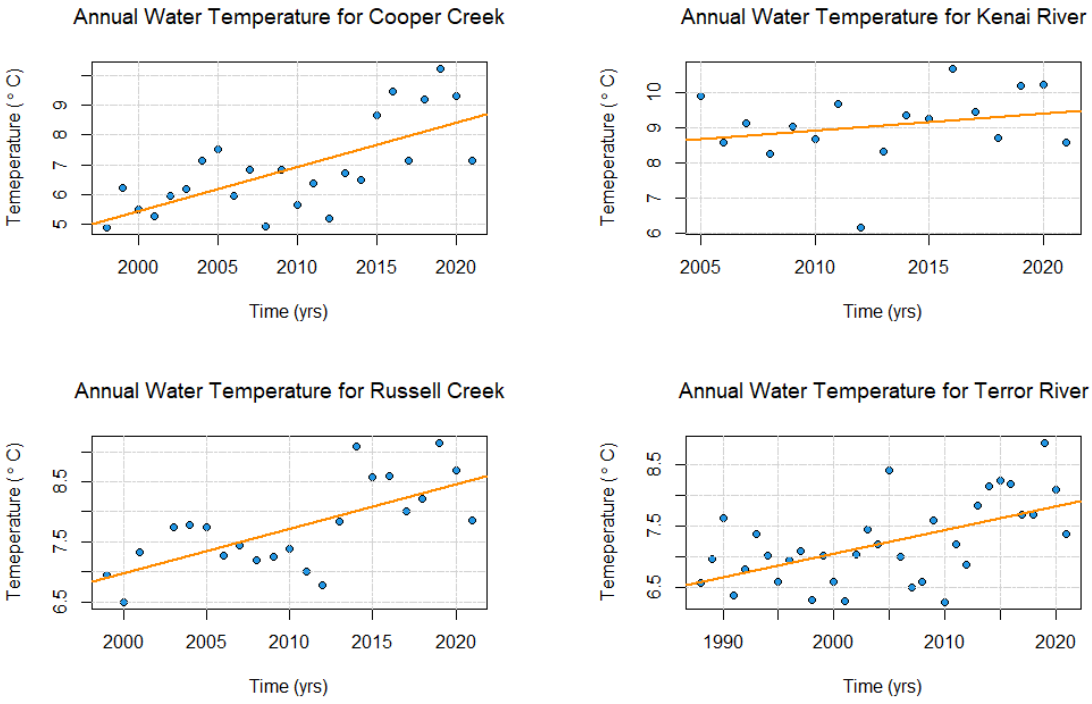

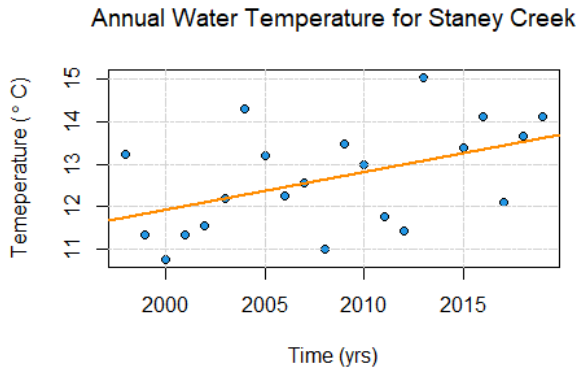

Figure 4.11: These are the water temperature trends for each river fitted with linear models.

Each of these plots follow closely to either a linear or sinusoidal trend. The mean of their slopes is 0.0797 °C per year. When fitting a linear model to Figure 4.10 the point estimate, or slope appears as 0.0803 °C per year, as shown below.

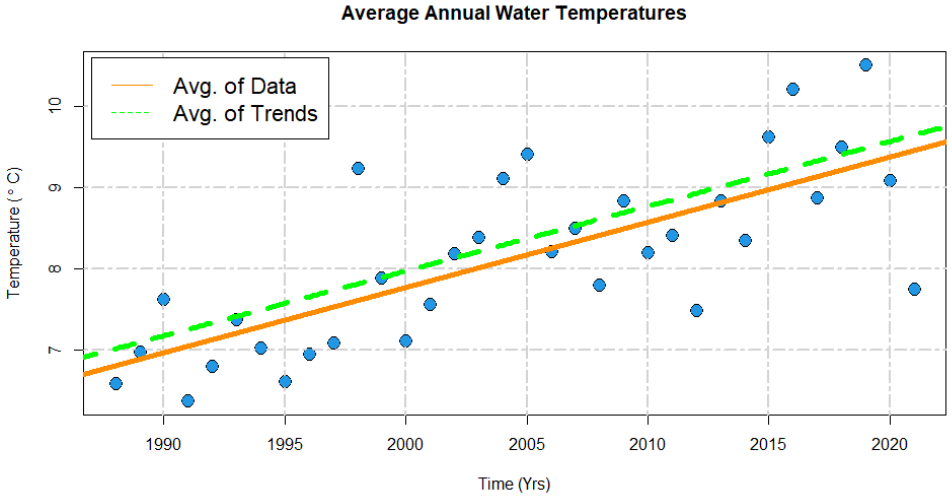

Figure 4.12: The solid line represents the trend of the average water temperature in Alaska for the past 33 years. The dashed line represents the average trend for each stream that was sampled in Alaska.

The figure above illustrates that for the past 33 years the change in Alaskan water temperature during the months of salmon spawning migration has a linear growth of approximately 0.08 °C per year. The model for the change in water temperature in Alaska can now be represented as:

$$T(t) = a * t + b, \tag{4.5}$$

with $a = 0.08$ and $b = -152.9$. The coefficient, a, represents the average growth of temperature over time, the intercept, b, represents the initial temperature of the water in Alaska about 2000 years ago, and t represents the time in years with an initial staring point 0 B.C. Obviously, the average temperature in Alaskan rivers and creeks 2000 years ago was not -152.9 °C, so the linear regression model is only useful for short time periods. Thus, letting $b = 9.54$ changes the initial starting time to the present year, 2022. Now, substituting the function $T(t)$ for parameter T in Equation (4.2) gives the below equation.

$$R(T(t)) = \ln\left(\frac{0.32 * 5}{1 + c(T(t) - T_{opt})^4}\right) = \ln\left(\frac{0.32 * 5}{1 + c(at + b - T_{opt})^4}\right). \tag{4.6}$$

Then substituting in all the variables will produce the below equation.

$$R(t) = \ln\left(\frac{0.32 * 5}{1 + 10^{-4}(0.08t - 2.96)^4}\right). \tag{4.7}$$

In Equation (3.3) the growth rate, r_x, was revealed after taking the derivative of Equation (3.2), so when applying the same method the below growth rate function is established.

$$\begin{aligned} \tfrac{d}{dt} x_0 e^{R(t)t} &= \left(R(t) + \tfrac{P'(t)t}{P(t)}\right) x_0 e^{R(t)t} \\ &= \left(R(t) + \tfrac{P'(t)t}{P(t)}\right) x, \end{aligned} \tag{4.8}$$

where

$$P(t) = \frac{0.32*5}{1+10^{-4}(0.08t-2.96)^4},$$

$$P'(t) = \frac{-4*0.32*5*10^{-4}*0.08(0.08t-2.96)^3}{(1+10^{-4}(0.08t-2.96)^4)^2} \tag{4.9}$$

$$= \frac{-5.12*10^{-4}(0.08t-2.96)^3}{(1+10^{-4}(0.08t-2.96)^4)^2}.$$

So, the growth rate function is now the equation below.

$$G(t) = R(t) + \frac{P'(t)t}{P(t)}. \tag{4.10}$$

To get a better understanding of what the growth rate function is doing, we graphed the function below.

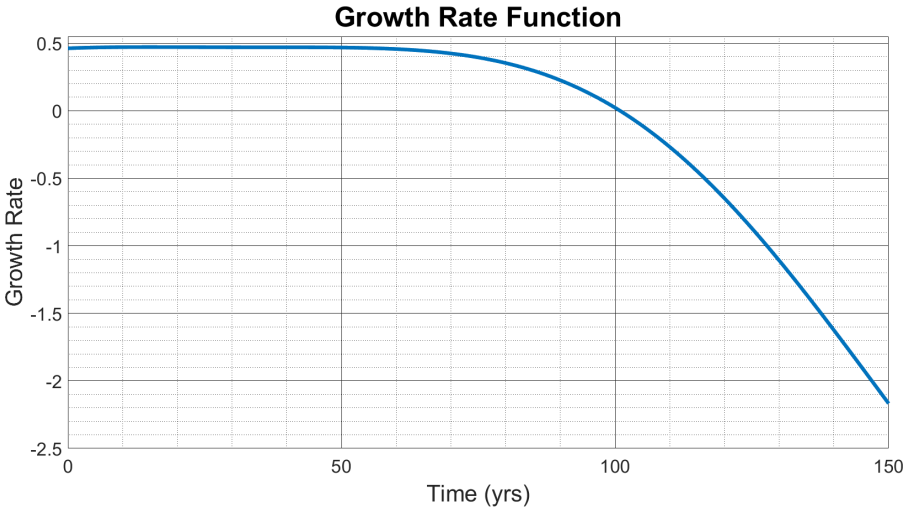

Figure 4.13: Plot of the growth rate function, Equation (4.10), over a time span of 150 years.

We can see in the figure above that the growth rate remains positive for approximately the first 100 years. After which, the growth rate becomes negative indefinitely. Now, we can substitute the above growth rate function into Equa-

tion (4.3), as shown below.

$$\frac{dx}{dt} = G(t)x\left(1 - \frac{x}{K_x}\right). \tag{4.11}$$

Since the model for the salmon population is now dependent on time it becomes a 2^{nd} order non-autonomous ordinary differential equation. When comparing this model to Equation (4.3), the below figure is produced.

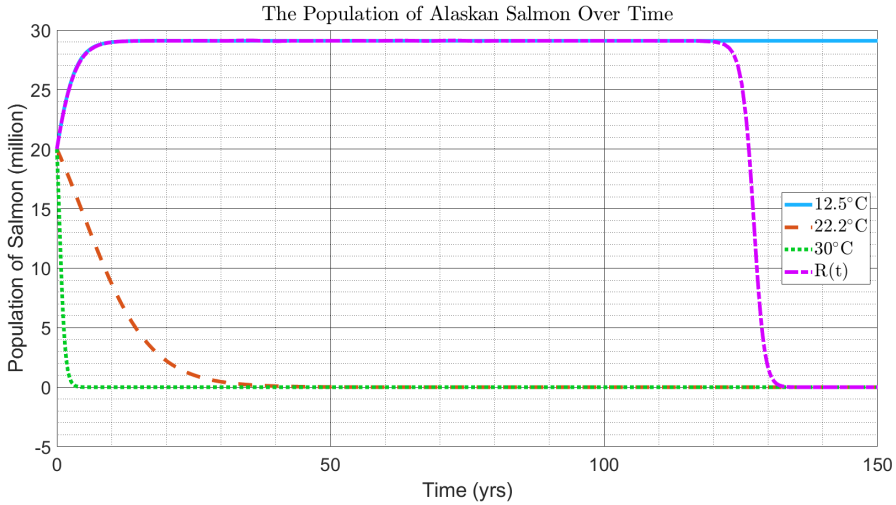

Figure 4.14: Compares solutions to the autonomous and non-autonomous logistic growth models, or Equation (4.3) and Equation (4.11).

Using the **vpasolve** function in MATLAB, we found that in approximately 101 years, the growth rate will change from positive to negative, which is the beginning of the population's descent. When substituting $t = 101$ into Equation (4.5), we get $T(101) = 17.62°\text{C}$. This temperature can be denoted as our inflection temperature for the salmon growth rate. From this figure, it is clear that the water temperature will be too hot for the salmon population in the future, resulting in their death.

Chapter 5

Including Interaction

We begin this chapter by introducing interaction terms, $c_{xy}xy$ and $c_{yx}xy$, which combine the salmon and brown bear growth models into a system of ordinary differential equations (ODEs). Next, a criteria is established for the parameters of the interaction terms, to ensure the behavior of the two species is similar to what we expect to observe in nature. The criteria is then used as a tool alongside the trace and determinant of the Jacobian matrix for picking interaction parameters, c_{xy} and c_{yx}. After that, we evaluate and plot the solutions to the system of ODEs where the temperature is constant. Lastly, in this chapter, we will conclude by comparing the system of ODEs where the temperature is constant and is a function of time.

5.1 Introducing Interaction

The models found in Equation (3.5) and Equation (4.3) are designed to individually represent the species' populations. This means that the outcome of one species does not affect the other. By including an interaction term in both models, we can simulate a trade-off, as we would see in the real world. We use Theodore

Modis' model, Equation (2.4), for inspiration in our own, as shown below.

$$\begin{aligned} \frac{dx}{dt} &= R(T)x\left(1-\frac{x}{K_x}\right) - c_{xy}xy, \\ \frac{dy}{dt} &= r_y y\left(1-\frac{y}{K_y}\right) + c_{yx}xy, \end{aligned} \tag{5.1}$$

where $c_x y,\ c_y x > 0$. Notice, for the salmon ODE, we subtract its interaction term, but for the brown bears we add its interaction term. We do this because the salmon population should have a negative consequence when there is an increase in brown bears. In contrast, the brown bears should be rewarded when their food source increases. The interaction parameters alter the affect of the carrying capacity, so we change $K_x = 15$ and $K_y = 5$ as a vague measure of their environmental limits. The parameters, c_{xy} and c_{yx}, control the stability of the populations, so they must be chosen carefully, to accurately represent the relationship between the species.

5.2 Picking Interaction Parameters

First, we look at the affects of c_{xy} and c_{yx} on the critical points of Equation (5.1). Before, finding the critical points of the system of ODEs, we fix the parameter, T, to the optimal temperature, 12.5°C, to eliminate the effect of temperature on the salmon population. Now, the equations can be rewritten as:

$$\begin{aligned} \frac{dx}{dt} &= R(T_{opt})x - \frac{R(T_{opt})x^2}{K_x} - c_{xy}xy, \\ \frac{dy}{dt} &= r_y y - \frac{r_y y^2}{K_y} + c_{yx}xy. \end{aligned} \tag{5.2}$$

Then, substituting $a_x = R(T_{opt})$, $b_x = \dfrac{R(T_{opt})}{K_x}$, $a_y = r_y$, and $b_y = \dfrac{r_y}{K_y}$ a similar model to Theodore Modis' model, Equation (2.4), is constructed.

$$\begin{aligned} \frac{dx}{dt} &= a_x x - b_x x^2 - c_{xy} xy, \\ \frac{dy}{dt} &= a_y y - b_y y^2 + c_{yx} xy. \end{aligned} \tag{5.3}$$

Now, we set the above system of equations equal to the $\vec{0}$.

$$0 = x(a_x - b_x x - c_{xy} y),$$

$$0 = y(a_y - b_y y + c_{yx} x).$$

Then, solving for x and y produces the critical points below.

$$x_1^* = 0, \quad y_1^* = 0,$$

$$x_2^* = K_x, \; y_2^* = 0,$$

$$x_3^* = 0, \quad y_3^* = K_y,$$

$$x_4^* = \tfrac{a_x b_y - c_{xy} a_y}{c_{xy} c_{yx} + b_x b_y} \;\; y_4^* = \tfrac{a_x c_{yx} + b_x a_y}{c_{xy} c_{yx} + b_x b_y}.$$

The first three critical points do not contain either of our unknown parameters, $c_{xy},\ c_{yx}$, but the fourth critical value does. Note, neither population can be negative and $c_{xy},\ c_{yx} > 0$, which creates the below criteria for these parameters.

$$0 < c_{xy} \leq \tfrac{a_x b_y}{a_y},$$

$$c_{yx} \geq -\tfrac{b_x a_y}{a_x}.$$

Since $a_x,\ b_x,\ a_y > 0$, then the criteria above changes to:

$$0 < c_{xy} \leq \tfrac{a_x b_y}{a_y},$$

$$c_{yx} > 0.$$

If we assume that $c_{yx} > c_{xy}$, this would imply that the rate at which salmon affect brown bears is higher than the rate at which brown bears affect salmon. However, brown bears eat a large quantity of salmon, but salmon do not have this direct

impact on bears. So, the brown bear population should have a higher affect on the salmon population. Therefore, the constraint for the parameters c_{xy} and c_{yx} is as follows.

$$0 < c_{xy} \leq \frac{a_x b_y}{a_y} = 0.104,$$
$$0 < c_{yx} < c_{xy}.$$

Now, assessing the eigenvalues of Equation (5.3) with the above constraint, will determine the stability around the critical point $(x_4^*,\ y_4^*)$. The eigenvalues can be found by solving for the characteristic polynomial of the Jacobian matrix for Equation (5.3).

$$J_{(x,y)} = \begin{pmatrix} a_x - 2b_x x - c_{xy} y & -c_{xy} x \\ c_{yx} y & a_y - 2b_y y + c_{yx} x \end{pmatrix}. \tag{5.4}$$

The characteristic polynomial of the above Jacobian matrix is displayed below.

$$\begin{aligned} \det(J_{(x,y)} - \lambda I) = \lambda^2 - \big[\ (a_x - 2b_x x - c_{xy} y) + (a_y - 2b_y y + c_{yx})\ \big]\lambda \\ + \big[\ (a_x - 2b_x x - c_{xy} y)(a_y - 2b_y y + c_{yx}) + c_{xy} x c_{yx} y\ \big]. \end{aligned} \tag{5.5}$$

Note that:

$$\begin{aligned} \mathrm{T} &= \mathrm{tr}(J_{(x,y)}) = (a_x - 2b_x x - c_{xy} y) + (a_y - 2b_y y + c_{yx}), \\ \mathrm{D} &= \det(J_{(x,y)}) = (a_x - 2b_x x - c_{xy} y)(a_y - 2b_y y + c_{yx}) + c_{xy} x c_{yx} y. \end{aligned}$$

So, substituting in the above variables in Equation (5.5) produces:

$$\det(J_{(x,y)} - \lambda I) = \lambda^2 - \mathrm{T}\lambda + \mathrm{D}.$$

Now, setting the above equation equal to zero and solving for our eigenvalues, λ, gives the below equation.

$$\lambda = \frac{\mathrm{T} \pm \sqrt{\mathrm{T}^2 - 4\mathrm{D}}}{2}.$$

As mentioned earlier, the stability for $(x_4^*,\ y_4^*)$ can be found by analyzing the eigenvalues. To achieve a stable oscillation the eigenvalues for the critical point

have to contain non-positive real parts and imaginary parts. This implies that $\mathrm{T} \leq 0$ and $\mathrm{T}^2 - 4\mathrm{D} < 0$. So for the critical point, $(x_4^*,\ y_4^*)$:

$$\mathrm{T} = \frac{a_y b_x (c_{xy} - b_y) - a_x b_y (b_x + c_{yx})}{b_x b_y + c_{xy} c_{yx}},$$

$$\mathrm{D} = \frac{(a_x c_{yx} + a_y b_x)(a_x b_y - a_y c_{xy})}{b_x b_y + c_{xy} c_{yx}}.$$

The values for the discriminant, $\mathrm{T}^2 - 4\mathrm{D}$, and trace, T, can be plotted by designing a meshgrid for the parameters c_{xy} and c_{yx} based on their constraints as shown below.

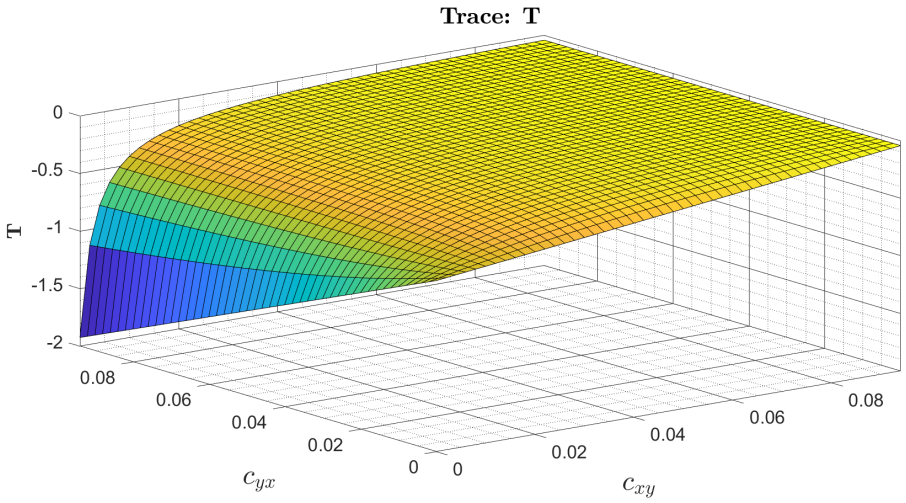

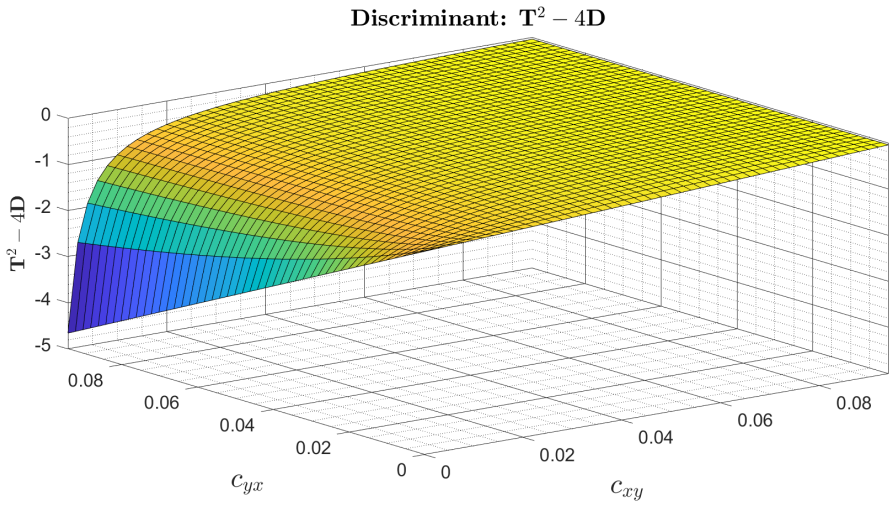

Figure 5.1: The graphs above are the trace and discriminant of $J_{(x_4^*, y_4^*)}$ for different values of the parameters c_{yx} and c_{xy}.

Notice that the values for the trace and discriminant are always negative for all c_{yx} and c_{xy} that belong in their constraints. Now, looking at these figure from a top-down view will provide a clear outline of which c_{yx} and c_{xy} values to test.

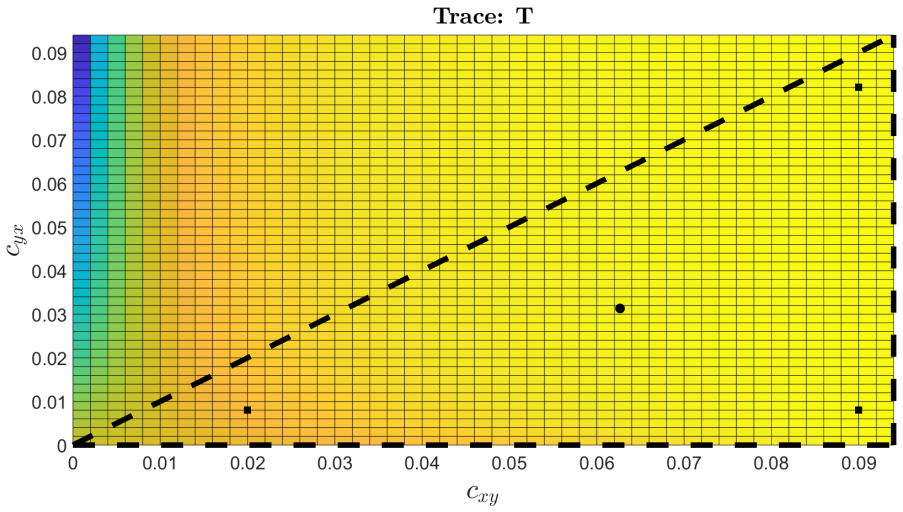

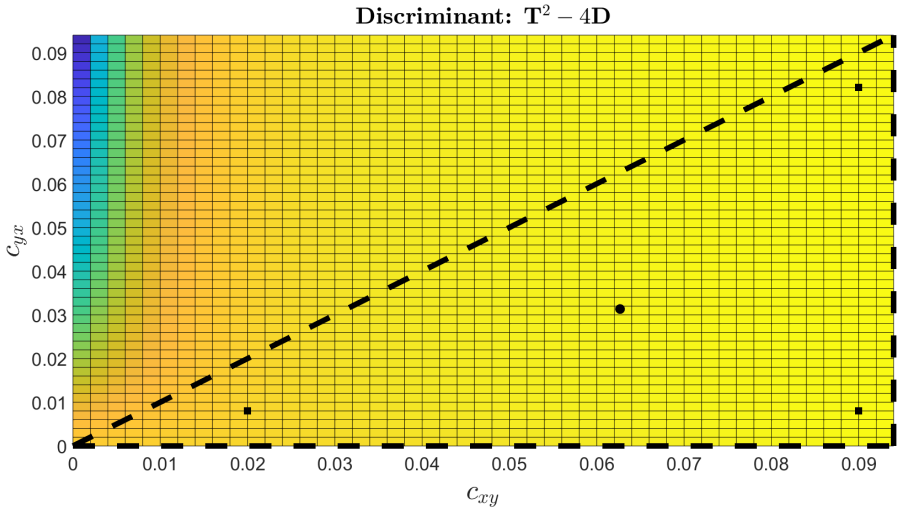

Figure 5.2: Top-down view of Figure (5.1). The points inside the right triangle are all values that satisfy the constraints of parameters c_{yx} and c_{xy}. The right triangle's center of mass is marked with a black dot at the coordinate point $(0.0696, 0.0348)$.

In the figure above a region is drawn where all c_{yx} and c_{xy} satisfy their constraints. Now, testing different c_{yx} and c_{xy} values will illustrate how different interaction rates will effect the outcome of the each species' population. The values chosen for $(c_{xy},\ c_{yx})$ are $(0.02,\ 0.008)$, $(0.09,\ 0.008)$, $(0.09,\ 0.082)$, and $(0.0627,\ 0.0313)$. These pair of interaction parameters can be seen plotted on the figure above. To compare each of the parameters, we plot the solutions to Equation (5.1), where the brown bear population is along the y-axis and the salmon population is along the x-axis as shown below for each pair of parameters.

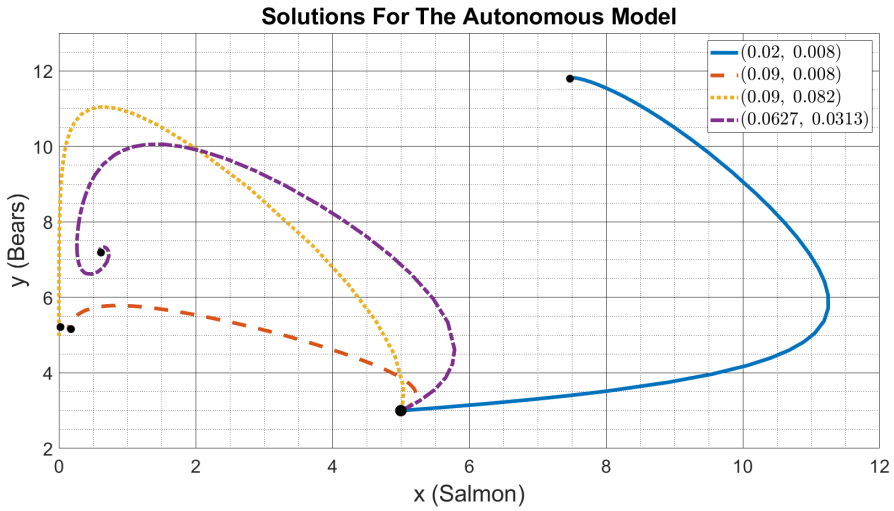

Figure 5.3: Compares the effect of different interaction rates on the autonomous model, Equation (5.1), where the initial conditions are $x_0 = 5$ and $y_0 = 3$.

The graph above shows that each of these parameters effects the location of the critical point, (x_4^*, y_4^*) as well as the oscillations of the populations. We chose the initial conditions, $x_0 = 5$ and $y_0 = 3$, to illustrate the dramatic difference in interaction parameters. When c_{xy} is large, the salmon population dies off, and when c_{yx} is large, the brown bear population increases faster before converging near its carrying capacity. Lastly, when the pair of parameters is equal to the right triangle's center of mass in Figure 5.2, the population oscillates and converges to its critical point $(0.61, 7.19)$. We will be using $c_{xy} = 0.0627$ and $c_{yx} = 0.0313$ to represent the interaction rates of the two species for Equation (5.1) because with these parameters the populations oscillate similar to what is expected in the real world. So, with all the parameters selected, the solutions to the autonomous model, Equation (5.1), with respect time is shown below.

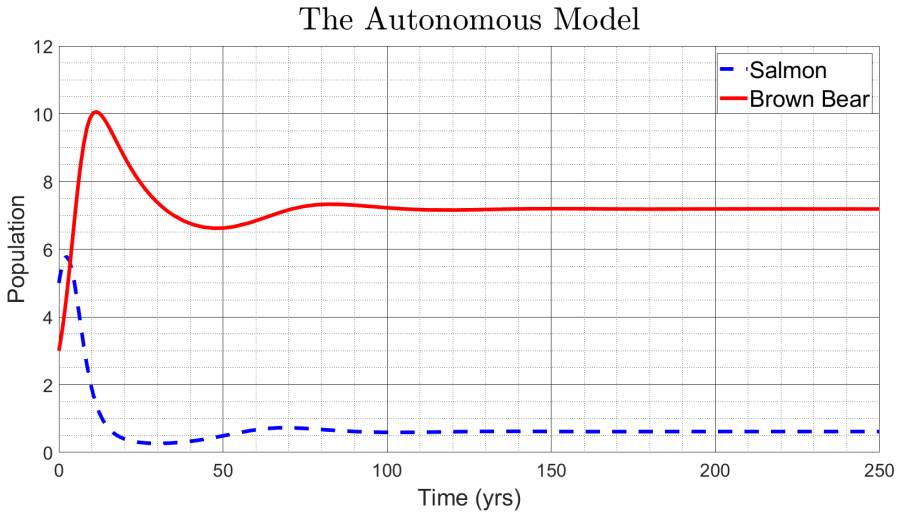

Figure 5.4: Plot of the solutions to the autonomous model, Equation (5.1), with respect to time.

In the figure above, both populations briefly increase before changing directions and oscillating toward their equilibrium points. Based on this figure, the brown bear population will quickly overtake the salmon population, bringing them near regional extinction. Now, we can compare these results to the system of ODEs, with the proposed growth rate, $G(t)$, shown below.

$$\begin{aligned} \frac{dx}{dt} &= G(t)x\left(1-\frac{x}{K_x}\right) - c_{xy}xy, \\ \frac{dy}{dt} &= r_y y\left(1-\frac{y}{K_y}\right) + c_{yx}xy. \end{aligned} \tag{5.6}$$

Now, using the same parameters for the autonomous model, Equation (5.1), we compare different initial conditions to analyze the stability of the model.

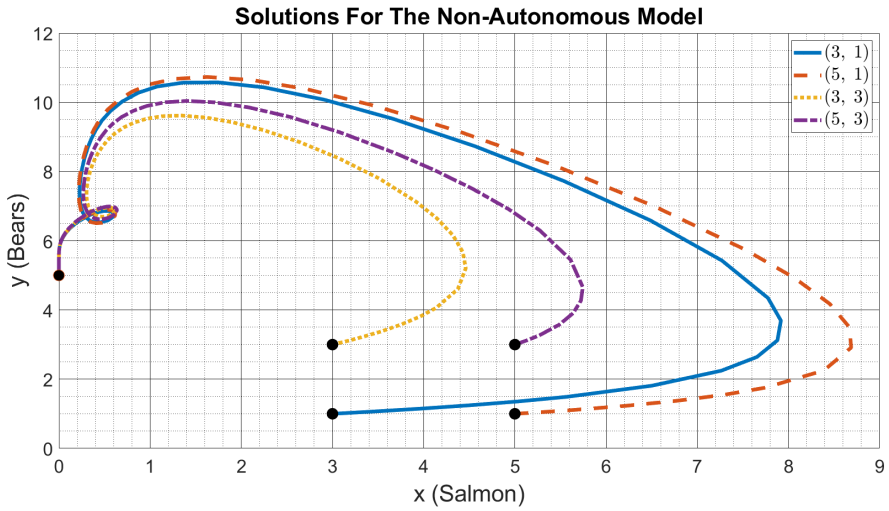

Figure 5.5: Compares the solutions to the non-autonomous model, Equation (5.6), with different initial conditions.

As expected the salmon population converges to zero as seen in Figure (4.14), resulting in the brown bear population converging to their carry capacity. When the salmon population dies off, the interaction terms in the model will approach zero and eventually the behavior of the brown bear species will be represented by its logistic equation, Equation (3.5). Lastly, in the graph below, we compare the results to the autonomous and non-autonomous model.

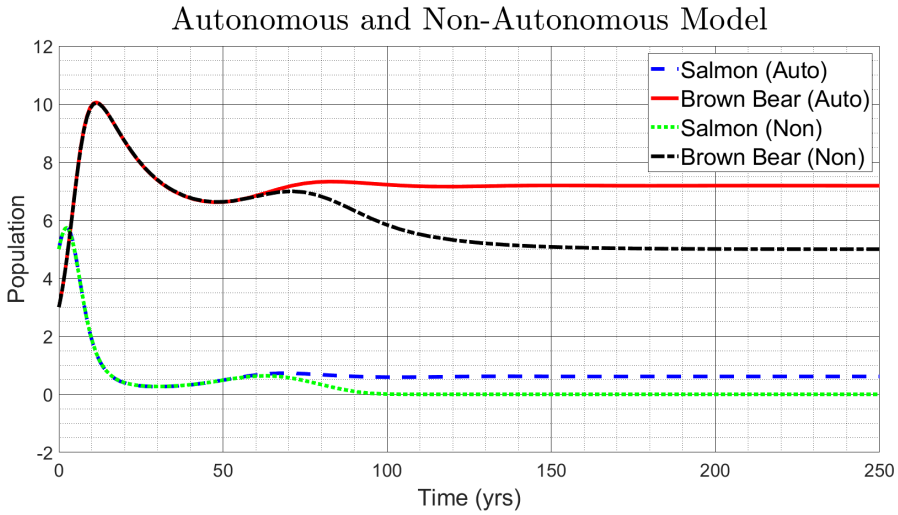

Figure 5.6: Plot of the solutions to the autonomous and non-autonomous model with respect to time.

Initially, the two models follow the same path, but after approximately 65 years, the curves begin to deviate. According to our temperature function, Equation (4.5), the projected Alaskan river temperature in 65 years is $T(65) \approx 14.7°\text{C}$. The graph illustrates that soon after the river temperature leaves the optimal range, the difference in model solutions becomes prominent. The non-autonomous model shows similar trends to the autonomous model, but ultimately resulting in the salmon population dying off and the Alaskan brown bear population converging to its carrying capacity.

Chapter 6

Conclusion

Bibliography

[Adams-Hosking et al., 2011] Adams-Hosking, C., Grantham, H. S., Rhodes, J. R., McAlpine, C., and Moss, P. T. (2011). Modelling climate-change-induced shifts in the distribution of the koala. *Wildlife Research*, 38(2):122–130.

[ADEC, 2018] ADEC (2018). Alaska greenhouse gas emissions inventory 1990-2015. `https://test.dec.alaska.gov/media/7623/ghg-inventory-report-overview-013018.pdf`. Accessed: April 3, 2022.

[ADFG, 2021] ADFG (2021). Brown/grizzly bear hunting in alaska, life history. *Alaskan Department of Fish and Game*.

[ADFG, 2022] ADFG, G. o. S. (2022). How water temperature affects development of young salmon. `https://www.adfg.alaska.gov/index.cfm?adfg=viewing.salmontemperature`. Accessed: July 17, 2022.

[Allchin, 2015] Allchin, D. (2015). Global warming: scam, fraud, or hoax? *The american biology Teacher*, 77(4):309–313.

[Anisiu, 2014] Anisiu, M.-C. (2014). Lotka, volterra and their model. *Didáctica mathematica*, 32:9–17.

[Barnes and Van Daele, 2010] Barnes, V. G. and Van Daele, L. J. (2010). Management of brown bear hunting on kodiak island, alaska. *Alaska Department of Fish and Game*, pages 1–30.

[Carter, 2005] Carter, K. (2005). The effects of temperature on steelhead trout, coho salmon, and chinook salmon biology and function by life stage. *California regional water quality control board*, pages 1–26.

[Crowley, 2000] Crowley, T. J. (2000). Causes of climate change over the past 1000 years. *Science*, 289(5477):270–277.

[Deacy et al., 2018] Deacy, W. W., Erlenbach, J. A., Leacock, W. B., Stanford, J. A., Robbins, C. T., and Armstrong, J. B. (2018). Phenological tracking associated with increased salmon consumption by brown bears. *Scientific reports*, 8(1):1–9.

[Elison et al., 2022] Elison, T., Tiernon, A., Sands, T., head, J., and Vega, S. (2022). 2021 bristol bay area annual management report. *Fishery Management Report*, 22-14:1–95.

[EPA, 2019] EPA, C. o. W. G. (2019). Overview of greenhouse gases. `https://www.epa.gov/ghgemissions/overview-greenhouse-gases`. Accessed: March 29, 2022.

[Farrell et al., 2008] Farrell, A., Hinch, S., Cooke, S., Patterson, D., Crossin, G. T., Lapointe, M., and Mathes, M. (2008). Pacific salmon in hot water: applying aerobic scope models and biotelemetry to predict the success of spawning migrations. *Physiological and Biochemical Zoology*, 81(6):697–708.

[Hansen et al., 2006] Hansen, J., Sato, M., Ruedy, R., Lo, K., Lea, D. W., and Medina-Elizade, M. (2006). Global temperature change. *Proceedings of the National Academy of Sciences*, 103(39):14288–14293.

[Hilderbrand et al., 1999] Hilderbrand, G. V., Jenkins, S., Schwartz, C., Hanley, T. A., and Robbins, C. (1999). Effect of seasonal differences in dietary meat intake on changes in body mass and composition in wild and captive brown bears. *Canadian Journal of Zoology*, 77(10):1623–1630.

[Hovey and McLellan, 1996] Hovey, F. W. and McLellan, B. N. (1996). Estimating population growth of grizzly bears from the flathead river drainage using computer simulations of reproduction and survival rates. *Canadian journal of Zoology*, 74(8):1409–1416.

[Lisi et al., 2013] Lisi, P. J., Schindler, D. E., Bentley, K. T., and Pess, G. R. (2013). Association between geomorphic attributes of watersheds, water temperature, and salmon spawn timing in alaskan streams. *Geomorphology*, 185:78–86.

[McLellan, 1989] McLellan, B. N. (1989). Dynamics of a grizzly bear population during a period of industrial resource extraction. iii. natality and rate of increase. *Canadian Journal of Zoology*, 67(8):1865–1868.

[Modis, 2011] Modis, T. (2011). Us nobel laureates: logistic growth versuvolterra–lotka. *Technological Forecasting and Social Change*, 78(4):559–564.

[NOAA, 2022] NOAA, N. C. f. E. i. (2022). Climate at a glance: Global time series. `https://www.ncdc.noaa.gov/cag/`. Accessed: April 3, 2022.

[NPS, 2020] NPS, G. o. S. (2020). Salmon monitoring in southwest alaska. `https://www.nps.gov/articles/salmonswan.htm#:~:`

text=Each%20year%2C%20up%20to%2060%20million%20sockeye%20salmon,State%20of%20Alaska%20is%20part%20of%20the%20answer. Accessed: July 11, 2022.

[Osterkamp and Lachenbruch, 1990] Osterkamp, T. and Lachenbruch, A. (1990). Thermal regime of permafrost in alaska and predicted global warming. *Journal of Cold Regions Engineering*, 4(1):38–42.

[Raftery et al., 2017] Raftery, A. E., Zimmer, A., Frierson, D. M., Startz, R., and Liu, P. (2017). Less than 2 c warming by 2100 unlikely. *Nature climate change*, 7(9):637–641.

[Ragan, 2015] Ragan, R. (2015). Alaska's five species of pacific salmon lifecycle and identification. *Alaskan Department of Fish and Game*.

[Stirling and Derocher, 2012] Stirling, I. and Derocher, A. E. (2012). Effects of climate warming on polar bears: a review of the evidence. *Global Change Biology*, 18(9):2694–2706.

[Taylor, 2008] Taylor, S. G. (2008). Climate warming causes phenological shift in pink salmon, oncorhynchus gorbuscha, behavior at auke creek, alaska. *Global Change Biology*, 14(2):229–235.

[Tsoularis and Wallace, 2002] Tsoularis, A. and Wallace, J. (2002). Analysis of logistic growth models. *Mathematical biosciences*, 179(1):21–55.

[UA, 2016] UA, C. o. W. G. (2016). Fact sheet - climate change - alaska.edu. https://www.alaska.edu/epscor/archive/phase-4/Salmon_2050/Fact-Sheet---Climate-Change.pdf. Accessed: April 3, 2022.

[UCAR, 2022] UCAR, C. o. W. G. (2022). Predictions of future global climate — center for science education. https://scied.ucar.edu/learning-zone/climate-change-impacts/predictions-future-global-climate. Accessed: April 3, 2022.

[USGS, 2022] USGS (2022). Usgs current water data for alaska. `https://waterdata.usgs.gov/ak/nwis/rt`. Accessed: April 3, 2022.

[Weber Scannell, 1992] Weber Scannell, D. P. K. (1992). Influence of temperature on freshwater fishes: A literature review with emphasis on species in alaska. `https://www.adfg.alaska.gov/static/home/library/pdfs/habitat/91_01.pdf`. Accessed: July 17, 2022.

[WFRC, 2022] WFRC, W. F. R. C. (2022). Questions and answers about salmon — u.s. geological survey. `https://www.usgs.gov/centers/western-fisheries-research-center/questions-and-answers-about-salmon`. Accessed: July 5, 2022.

[Wiig et al., 2008] Wiig, Ø., Aars, J., and Born, E. W. (2008). Effects of climate change on polar bears. *Science Progress*, 91(2):151–173.

Appendices

Appendix A

TABLES

Sockeye Comparison Between Weight and Run Size in Bristol Bay

Table A.1: Comparing the average weight of sockeye salmon to their run size in Bristol Bay each year. The data used to make this table was taken from the "*2021 BRISTOL BAY AREA ANNUAL MANAGEMENT REPORT*" [Elison et al., 2022].

Year	Weight (lbs)	Run (mil)
2001	6.7	22.3
2002	6.1	16.9
2003	6.3	24.9
2004	5.8	41.9
2005	6.3	39.3
2006	5.7	42.9
2007	5.8	44.8
2008	5.8	40.4
2009	5.9	40.4
2010	5.5	40.6
2011	6.2	30.6
2012	5.7	30.4
2013	6.0	24.4
2014	5.6	41.1
2015	5.2	58.8
2016	5.4	51.7
2017	5.5	57.6

Continued on next page

Table A.1 – continued from previous page

Year	Weight (lbs)	Run
2018	5.1	63.0
2019	5.1	56.4
2020	5.1	58.3
2021	4.7	67.7

Volume of Sockeye Salmon Runs Each Year in Bristol Bay

Table A.2: Using Table A.1 to calculate the volume for each year.

Year	Volume (MMCF)
2001	3.41
2002	2.35
2003	3.58
2004	5.55
2005	5.65
2006	5.58
2007	5.93
2008	5.35
2009	5.44
2010	5.1

Continued on next page

Table A.2 – continued from previous page

Year	Volume (MMCF)
2011	4.33
2012	3.96
2013	3.34
2014	5.25
2015	6.98
2016	6.37
2017	7.23
2018	7.34
2019	6.57
2020	6.79
2021	7.26

Average Annual Harvest For Salmon in Bristol Bay

Species	**Harvest**
Sockeye	28,100,000
Chinook	39,571
Chum	1,100,000
Coho	95,583
Pink	510,000
Total	**29,845,154**

Table A.3: Average annual commercial harvest for each salmon species from (2001−2020) [Elison et al., 2022]. Pink Salmon are reported in even years because of their two year life cycle pattern.

Appendix B

CODE

Jacobian Matrix Code

```
% Jacobian of The Model

clc
format rational


r_S = 5;
c = .0001;
T_opt = 12.5;

R =@(T) log( .32*r_S / ( 1 + c*(T - T_opt)^4 ) );

T = 12.5;

a1 = R(T);
b1 = a1 / 15;
c1 = .04;
```

```
18 a2 = -.016123;
19 b2 = a2 / 6;
20 c2 = .00008;
21
22 fprintf('The water temperature will remain constant at T=%.1f\n\n',
       T)
23 % Jacobian for critical point (0,0)
24 fprintf('The Jacobian for the critical point (0,0) is:')
25 J_1 = [a1, 0; 0, a2];
26 display(J_1)
27
28     % Eigenvalues of J_1
29 fprintf('The eigenvalues of the Jacobian above are:\n')
30 disp(eig(J_1))
31
32 % Jacobian for critical point (0,K_2)
33 fprintf('The Jacobian for the critical point (0,%d) is:',a2/b2)
34 J_2 = [a1-c1*a2/b2, 0; c2*a2/b2, -a2];
35 display(J_2)
36
37     % Eigenvalues of J_2
38 fprintf('The eigenvalues of the Jacobian above are:\n')
39 disp(eig(J_2))
40
41 % Jacobian for critical point (K_1,0)
42 fprintf('The Jacobian for the critical point (%.0f,0) is:',a1/b1)
43 J_3 = [-a1, -c1*a1/b1; 0, a2+c2*a1/b1];
44 display(J_3)
45
46     % Eigenvalues of J_3
```

```
fprintf('The eigenvalues of the Jacobian above are:\n')
disp(eig(J_3))

% Jacobian for critical point (x*,y*)
x_star = (a1*b2 - c1*a2) / (c1*c2 + b1*b2);
y_star = (a1*c2 + b1*a2) / (c1*c2 + b1*b2);
fprintf('The Jacobian for the critical point (%f,%f) is:',[x_star,
    y_star])
J_4 = [(-a1*b1*b2+2*b1*c1*a2-b1*c1*a2) / (c1*c2 + b1*b2),...
    (-a1*c1*b2 + c1^2*a2) / (c1*c2 + b1*b2);...
    (a1*c2^2 + b1*a2*c2) / (c1*c2 + b1*b2),...
    (-a2*b1*b2 - 2*a1*b2*c2 + a1*b2*c2) / (c1*c2 + b1*b2)];
display(J_4)

    % Eigenvalues of J_4
fprintf('The eigenvalues of the Jacobian above are:\n')
disp(eig(J_4))
```

Logistic ODE Code

```
clc
clear
close all

r = .01;
K = 10;
N = 0:.1:K+1;
y = r.*N.*(1-N./K);
plot(N,y,'LineWidth',4)
ax = gca;
```

```
ax.GridAlpha = 1;
set(gca,"FontSize",20)
set(gca,'XTickLabel',[],'YTickLabel',[])
grid on
grid minor
ax.MinorGridAlpha = 1;
xlim([0,11])
ylim([-.015,.03])
xlabel('\textbf{$x$}','Interpreter','latex','FontSize',25)
ylabel("\textbf{$x$}$'$","Interpreter','latex","FontSize",25)
title("\textbf{$x$}$'$ versus \textbf{$x$}","Interpreter',...
    'latex',"FontSize",25)
```